INTER-AMERICAN TROPICAL TUNA COMMISSION

2nd REVIEW OF THE STOCK ASSESSMENT OF BIGEYE TUNA IN THE EASTERN PACIFIC OCEAN

La Jolla, California (USA)
11-15 March 2019

DOCUMENT WSBET-02-08

INVESTIGATING POTENTIAL CAUSES OF MISSPECIFICATION-INDUCED REGIME SHIFT IN RECRUITMENT IN THE EPO BIGEYE TUNA ASSESSMENT

Juan L. Valero, Mark. N. Maunder, Haikun Xu, Carolina Minte-Vera, Cleridy Lennert-Cody and Alexandre Aires-da-Silva

CONTENTS

1. INTRODUCTION 3
1.1. Hypothesis for recruitment shift 4
1.1.1 Spatial mismatch 4
1.1.2 Growth misspecification 5
1.1.2.1 Wrong specification of Richards growth curve 5
1.1.2.2 Wrong growth curve model 5
1.1.3 Length-Weight relationship misspecification 5
1.1.4 Short time model time span 5
1.1.5 Selectivity misspecification 5
1.1.6 Catchability misspecification 6
1.1.7 Problems in the longline CPUE standardization 6
1.2 Objectives 6
2. METHODS 6
2.1. General approach 6
2.1.1 Spatial mismatch 6
2.1.2 Growth misspecification 7
2.1.2.1 Wrong specification of Richards growth curve 7
2.1.2.2 Wrong growth curve model 7
2.1.3 Length-Weight relationship misspecification 7
2.1.4 Model time span 8
2.1.5 Selectivity misspecification 8
2.1.6 Catchability misspecification 8
2.1.7 Problems in the longline CPUE standardization 8
3. RESULTS AND DISCUSSION 8
3.1.1 Spatial mismatch 8
3.1.2 Growth misspecification 9

3.1.2.1 Wrong specification of Richards growth curve 9
3.1.2.2 Wrong growth curve model 10
3.1.3 Length-Weight relationship misspecification 10
3.1.4 Model time span 10
3.1.5 Selectivity misspecification 10
3.1.6 Catchability misspecification 11
3.1.7 Problems in the longline CPUE standardization 11
4. CONCLUSSIONS 11
5. REFERENCES 13
TABLES 15
FIGURES 19

1. INTRODUCTION

Bigeye tuna (*Thunnus obesus*) are distributed across tropical to temperate oceanic waters of the Pacific Ocean, although the largest catches are taken towards the eastern and western ends of the ocean basin (Figure 1). Bigeye has been a primary target of Japanese longline fisheries since the 1950s (Miyabe and Bayliff 1998; Miyake *et al*. 2004), and prior to 1994 the longline fishery took about 90% of the total catch. However, with the development of the purse-seine fishery on fish-aggregating devices (FADs) in the mid-1990s, directed mainly at skipjack tuna (*Katsuwonus pelamis*), purse-seine catches rose dramatically, from 10% or less to 60% or more of the total in a two-year period (Figure 2; Fonteneau *et al*. 2013). There are important differences between the two fisheries in the length composition of their catches (Figure 3) and in their areas of operation. Purse seines catch mostly small bigeye, primarily between 5°N and 5°S, whereas longline catches, which consist of large fish, are distributed more continuously geographically, but are relatively low between 160°W and 180° (Schaefer *et al*. 2015). In the eastern Pacific Ocean (EPO), bigeye are rarely caught by purse seiners north of 10°N, but a portion of the longline catches of bigeye is taken north of that parallel (Aires-da-Silva *et al*. 2017).

The current stock assessment of bigeye in the EPO (Aires-da-Silva *et al*. 2017) assumes a single stock. Although this single-unit stock model is not spatially structured, it accounts for spatial structure to some extent by using a "fleet-as-areas" approach (see, for example, Cope and Punt 2011; Hurtado-Ferro *et al*. 2014), which assumes several fisheries that are defined by partitioning the data in space and act on the stock with different catchabilities and selectivities. The underlying assumption of this approach is that the bigeye stock is randomly mixed within the EPO, with no localized spatial dynamics, except possible spatial partitioning by age.

Bigeye movements and potential stock structure in the EPO have been discussed by Schaefer (2009), Schaefer and Fuller (2009), and Schaefer *et al*. (2015). Analyses of conventional and archival tag data indicate constrained dispersion in latitude, some regional fidelity, and extensive eastward longitudinal dispersion (Schaefer *et al*. 2015). One of the areas of higher site fidelity and "viscosity" (the tendency of fish to stay in a particular area, as opposed to dispersion; see Schaefer *et al*. 2015) in movements is the equatorial EPO between approximately 90°W and 115°W (Schaefer and Fuller 2009; Schaefer *et al*. 2015) (Figure 4).

A recurrent feature of bigeye assessments in the EPO since 2003 (Harley *et al*. 2005; Fonteneau and Ariz 2008; Aires-da-Silva 2017) is a sudden increase in the estimated recruitment starting in the mid-1990s, and resulting in an apparent "two-regime" pattern in recruitment, with estimates after 1995 about double those before that year (Figure 5). Although this pattern mostly disappeared in the 2014 assessment (Aires-da-Silva and Maunder 2014), it resurfaced in subsequent assessments. Several hypotheses have been proposed to explain this pattern (Aires-da-Silva *et al*. 2010), including an environmental regime shift (Fonteneau and Ariz 2008), underestimated floating-object catches for the period prior to 1994 (Fonteneau and Ariz 2008), higher natural mortality rates than those assumed in the assessment models (Fonteneau and Ariz 2008), density-dependent growth (S. Hoyle, pers. comm.), changes in migratory patterns (S. Harley, pers. comm.), and a modeling artifact caused by the large catches of small individuals by the purse-seine fishery (Maunder *et al*. 2010). Although any of these hypotheses might account for the two-regime recruitment pattern, only some of them have been evaluated, and their plausibility remains in question. To date, two analyses have corrected the pattern: first, allowing what were previously considered unrealistically high natural mortalities for medium and large bigeye (Maunder *et al*. 2010), and second, a "spatial mismatch" hypothesis (Aires-da-Silva *et al*. 2010; Valero *et al*. 2018), which postulates that the pattern could be explained by a spatial mis-specification in the assessment model that ignores local depletion. This hypothesis is described in the next section.

1.1. Hypothesis for recruitment shift

1.1.1 Spatial mismatch

Under this hypothesis, the two-regime pattern is the result of a spatial mis-specification in the stock assessment model; in other words, it is an artifact of the model, caused by the assumption that bigeye in the EPO form a single homogeneous stock. This hypothesis seems to be consistent with major historic events in the bigeye fishery in the EPO. In particular, the estimated recruitment shift coincided with the very rapid expansion of the purse-seine fishery on FADs in the equatorial EPO in the mid-1990s. This resulted in competition with the longline fishery, which had operated along the equatorial grounds for several decades. Decreased longline catch rates (see Aires-da-Silva and Maunder 2010) and apparent gear conflicts between longline and purse-seine fisheries (see, for example, Skillman *et al*. 1993) resulted in a gradual exodus of longliners from the central equatorial fishing areas towards the west, south, and north. Longliners may also have shifted their fishing effort to less-exploited fishing grounds or to distinct sub-stocks of bigeye in the EPO after the mid-1990s. Preliminary spatial analyses of historical changes in the distribution of longline and purse-seine effort, and some anecdotal information, support this series of historic events. Also, the evidence of restricted movements and limited mixing of bigeye in the equatorial EPO from tagging data (Figure 4) (Schaefer and Fuller 2009; Schaefer *et al*. 2015) suggests that juvenile bigeye exploited by the FAD fishery may not become vulnerable later in life to longliners in those newly-occupied fishing grounds. This would also account for the fact that the increase in purse-seine catch does not appear to reduce the longline CPUE, and hence the index of relative abundance, since the longline CPUE index measures abundance over a wider, or different (Figures 1 and 6), area than where the increased purse-seine catch occurred.

If the spatial mismatch hypothesis is correct, a spatially-structured bigeye assessment should minimize, or even eliminate, the two-regime recruitment pattern. Aires-da-Silva and Maunder (2010) tested the impact of this hypothesis on the results of the bigeye assessment by fitting spatially disaggregated and independent models for four areas of the EPO (Figure 6), resulting in different trends and depletion levels among areas and a partial correction of the two-regime pattern, which is desirable to remove model misspecification and potential model biases. Valero *et al.* (2018) conducted a similar spatially disaggregated integrated age-structured model approach but restricted to the Central area outlined in Aires-da-Silva and Maunder (2010) (Figure 6) and found a steeper declining trend in the spawning biomass ratio (the ratio of the spawning biomass of the current stock to that of the unfished stock; SBR), and a more depleted stock status in the Central area than is estimated by the base case stock assessment for the whole EPO. Recruitment estimates for the Central area did not show the two-regime pattern typical of previous models. These results were consistent with those of Aires-da-Silva and Maunder (2010). However data was not available to repeat the same configuration used in Aires-da-Silva and Maunder (2010) until a later date, results of such comparison is available in Valero *et al.* (2019) showing a return of the estimated recruitment shift.

Valero *et al.* (2018) also systematically explored the effect of alternative spatial configurations on model results, three latitudinal bands (5°N-5°S, 10°N-5°S and 10°N-10°S) and four longitudes (95°W, 100°W, 110°W, and 120°W) were used to divide the EPO into 12 six-area grids, for a total of 72 individual areas. An independent (*i.e*. no movement among areas nor sharing of estimated parameters) age-structured production model (ASPM) was fitted for each area, using area-specific total catches aggregated by fleet (purse-seine and longline) and nominal (unstandardized) longline CPUE. For most of the twelve possible six-area combinations, some of the areas had too few or too sparse data for meaningful results, especially the inshore areas north and south of the equatorial areas, and to a lesser extent the areas north and west of the equatorial areas (See Valero *et al.* 2018). This suggested that, in a systematic division of the EPO at least, six areas are too many, and that fewer areas, or defining spatial areas by other criteria

(see Lennert-Cody *et al.* 2010, 2013; Minte-Vera *et al.* 2019) may perhaps be a better approach to delineate spatial areas. For area combinations with enough data, there was general consistency in the results, with larger biomass declines in the equatorial areas, while the other areas showed either flat biomass trajectories or lesser declines. Overall results indicate that the two-regime recruitment pattern appears in several of the area combinations if the ASPM is used, indicating that the recruitment pattern is independent of length compositions, which were not used in the ASPM.

1.1.2 Growth misspecification

1.1.2.1 Wrong specification of Richards growth curve

Growth in the EPO bigeye tuna assessments has been modeled using a Richards growth model (for more details see the Growth document off the BET review, Anonymous, 2019). The parameterization of the Richards growth curve in Stock Synthesis is fit to the quarterly estimates of mean length at age from the growth curve estimated by Aires da Silva et al. (2015) to estimate the parameters to use in the stock assessment (Table 1).Maybe growth is wrongly estimated. Performed runs with estimated growth, either Linf or CVs or all growth parameters.

1.1.2.2 Wrong growth curve model

Although the Richards growth curve is more flexible than the traditional von Bertalanffy growth curve used in earlier BET models, there is evidence that it may not be flexible enough for BET growth, particularly for the few large size tagged BET recovered (Anonymous 2019). Maunder *et al.* (2018) developed the Growth Cessation Model and found that it fits better to the data than the Richard's curve.

1.1.3 Length-Weight relationship misspecification

Models have used a length-weight relationship estimated by Nakamura and Uchiyama (1964) which is based upon over 9,000 individuals from the longline fishery, mainly medium to large tuna ranging in length from 80 to 190 cm. In addition to its use in the stock assessment models, this relationship is used to estimate purse-seine catches. However purse-seine catches are mainly small and medium tuna from 30-150 cm. Harley *et al*. (2005) suggested that the relationship of Nakamura and Uchiyama (1964) may overestimate the weights of small and medium (50-100 cm) bigeye by 10-15%. This is because small fish were not included in the study of Nakamura and Uchiyama and thus predictions of the weights of smaller individuals are outside the range of the observed data. This could have implications for both the stock assessment and the estimation of purse seine catches from the species-composition sampling.

1.1.4 Short time model time span

The current models used for providing BET management advice start in 1975, however there is data from 1950s. Since there was exploitation before 1975, the BET the base case model and other model sensitivities to date include the estimation of initial fishing mortality at equilibrium. The initial F is estimated without fitting to an initial equilibrium catch by given the initial catch a lambda of 0. Therefore the initial F is estimated by the other data types, mainly the length composition data. There is the potential for some model issues if other processes (such as growth, selectivity and natural mortality) are misspecified that may affect the initial F and the level of depletion.

1.1.5 Selectivity misspecification

The BET base case model uses a length-based selectivity, which is asymptotic for the longline fisheries. Perhaps an age-based selectivity could perform better. Also there may be some degree of dome-shaped selectivity if larger/older bigeye tuna are less vulnerable to the longline fisheries by for example going deeper in the water column with age/size.

1.1.6 Catchability misspecification

Either catchability may have changed in the mid 1990s due to the expansion of FAD fisheries, or there may be hyperdepletion or hyperstability in catchability if the longline index is not proportional to biomass. This potential issues has not been evaluated in the BET assessment.

1.1.7 Problems in the longline CPUE standardization

The only index of abundance the BET base case assessment has been fitted to it is the Japanese CPUE longline index. However there are other longline fleets that fish for BET and recent work (see recent longline IATTC Workshop) has provided alternative uses of data and standardization approaches.

1.2 OBJECTIVES

Identifying potential sources of the two-regime pattern in the bigeye assessment, particularly if it is due to model misspecification, is important not only for purposes of the stock assessment but also for the ongoing management strategy evaluation (MSE) work at the IATTC (Maunder *et al*. 2016), since the operating model for MSE work is based on the stock assessment model. Realistic operating models are of paramount importance for conducting MSE work, and it is desirable to eliminate potential model misspecification, and the resulting potential bias, in stock assessments to improve the accuracy of the management advice based on such assessments.

This report presents the results of alternative model configurations and uses of data under different hypotheses to investigate potential causes of the regime shift in recruitment in the BET assessment. The main assumption is that the estimated regime shift in recruitment is a result of model misspecification rather than actual shift in recruitment. Although alternative spatial configurations were evaluated as part of this effort, they are reported elsewhere in more detail (Valero *et al.* 2019). The main objective is to evaluate the impact of alternative model configurations on the bigeye assessment, and to determine which configurations remove the two-regime recruitment pattern.

2. METHODS

2.1. GENERAL APPROACH

Alternative integrated model runs were conducted with the modeling platform Stock Synthesis (SS). Since the latest BET base case assessment model is run with SS version 3.23b (compiled November 2011) some of the alternative models based on the base case were conducted using SS 3.23b, however most of the alternative models were implemented in version 3.3.12 (compiled September 2018). A comparison of BET base case model run results using both versions is available (Valero 2019) as part of the information papers for the BET review workshop. Table 1 is an overview of main configuration differences between the current BET base case assessment model and alternative models.

Since the main goal is to evaluate the impact of alternative model configurations on the bigeye assessment, and to determine which configurations remove the two-regime recruitment pattern we set up alternative models under different hypothesis and report key model results such as comparisons of estimated biomass trajectories and a simple statistic of the magnitude of the two-regime recruitment pattern. This statistic (R_{shift}) is the ratio of the median age-0 recruitment after the expansion of the FAD fishery (year 1994) over the median age-0 recruitment before the FAD expansion.

2.1.1 Spatial mismatch

Alternative models were implemented under different assumptions about spatial structure in EPO BET dynamics. Data was partitioned across the spatial boundaries described above and longline indices were computed for each of the area combinations. The rational for spatial structure assumptions can be

found on Minte-Vera *et al.* (2019). Several alternative spatial partitions of the EPO were evaluated:

1) "Default": This corresponds to the spatial structure configuration described in Minte-Vera et al. (2019), see Figure 7.

2) "Alternative 1": Based on the "Default" spatial partition, but further dividing the offshore equatorial area at 130W into two areas, see Figure 8.

3) "Alternative 2": Based on the "Default" spatial partition, but further dividing the offshore equatorial area at the equator into two areas, see Figure 9.

4) "Alternative 3": Following the spatial structure used in Aires-da-Silva and Maunder (2010), except their coastal component (see Figure 6) has been merged with the other areas along their latitude borders, see Figure 10.

For the "Default" spatial configuration, different models were implemented including:

a) 4-area model with no movement

b) 4 separate models (one for each area)

c) 4-area model with an age-invariant eastward movement rate of 16% per quarter (Figure 11)

d) 4-area model with an age-dependent eastward movement rate at 16% per quarter for only juveniles (aged 3 to 8 quarters), no movement for the other ages (Figure 12)

e) 4-area model with an age-dependent eastward movement rate at 16% per quarter only juveniles (aged 3 to 8 quarters) and 5% per quarter diffusion for BET aged 15 quarters and older (Figure 13)

For "Alternative 1" and "Alternative 2" we focused only on the further divisions for Area 1 (offshore equatorial, Figure 8 ad Figure 9), since preliminary results indicated that Area 1 was where the recruitment shift in recruitment was evident (see Figure 15).

For "Alternative 3" a three-area model with no movement was implemented.

2.1.2 Growth misspecification

2.1.2.1 Wrong specification of Richards growth curve

Maybe growth is wrongly estimated. Performed runs estimating parameters of the Richards growth curve currently used in the BET base case model, either Linf, K of the variation of size at age or all growth parameters jointly. Alternative model runs were conducted for the area A1 of the "Default" spatial structure and for the current base case BET assessment.

2.1.2.2 Wrong growth curve model

We tried a growth cessation model (Maunder *et al.* 2018) as an alternative to the Richards growth curve used in the base case model with a beta version of SS (version 3.3.13_beta).

2.1.3 Length-Weight relationship misspecification

Models have used a length-weight relationship estimated by Nakamura and Uchiyama (1964) which is based upon over 9,000 individuals from the longline fishery, mainly medium to large tuna ranging in length from 80 to 190 cm. In addition to its use in the stock assessment models, this relationship is used to estimate purse-seine catches. However purse-seine catches are mainly small and medium tuna from 30-150 cm. Harley *et al*. (2005) suggested that the relationship of Nakamura and Uchiyama (1964) may overestimate the weights of small and medium (50-100 cm) bigeye by 10-15%. This is because small fish were not included in the study of Nakamura and Uchiyama and thus predictions of the weights of small-

er individuals are outside the range of the observed data. This could have implications for both the stock assessment and the estimation of purse seine catches from the species-composition sampling. We estimated an alternative L-W relationship using 379 paired length-weight observations from BET caught with purse-seine gear (Dan Fuller and Kurt Schaeffer, IATTC, Pers. Comm.).

2.1.4 Model time span

The current models used for providing BET management advice start in 1975, however there is data from 1950s. Available data include catches and digitized longline size frequency distributions from longline from 1958 to 1963 from Kume and Joseph (1966). Alternative SS models were implemented starting back to 1954.

2.1.5 Selectivity misspecification

The BET base case model uses a length-based selectivity, which is asymptotic for the longline fisheries. Perhaps including an age-based selectivity could allow for modeling of changing availability of fish of different ages. To explore this possibility, model runs were conducted using both length-based and age-based selectivity for area A1 of the "Default" BET spatial structure.

Alternatively, there may be some degree of dome-shaped selectivity if larger/older BET are less vulnerable to the longline fisheries by for example going deeper in the water column with age/size. Runs were conducted allowing for dome shape length-based selectivity for the longline fishery for area A1 of the "Default" BET spatial structure.

2.1.6 Catchability misspecification

Alternative runs were set up in order to explore potential catchability changes in the mid 1990s due to the expansion of FAD fisheries. Hyperdepletion or hyperstability in the longline fishery was also evaluated to explore if there is support for the longline index not being proportional to biomass.

2.1.7 Problems in the longline CPUE standardization

The only index of abundance the BET base case assessment has been fitted to it is the Japanese CPUE longline index. However there are other longline fleets that fish for BET and recent work has provided alternative use of data and standardization approaches. We implemented alternative SS model runs using different longline indices for area A1 of the "Default" spatial structure, including indices based on small spatial scale operational data from longline operations, standardizations that take into account a vessel effect and a hook-per-basket covariate and the aggregated in a 5x5 degree grid like in the base case.

3. RESULTS AND DISCUSSION

3.1.1 Spatial mismatch

The 4-area model with no movement for the "Default" spatial structure provided reasonably good fits to the indices of abundance and length composition data (Figure 14). However, the recruitment shift is still evident (Figure 15) in a similar magnitude as the base case model (Figure 16). The 4 independent area models produced similar combined results, as expected, and helped highlight area A1 (Offshore equatorial, Figure 7) as the apparent source of the regime shift with a R_{shift} = 2.44, with the other areas little (A2 and A3 R_{shift} = 1.3) or no change in recruitment levels (A4 R_{shift} = 0.96)(Figure 17).

Alternative models for the "Default" spatial structure with different assumptions regarding BET movement reduce or remove the recruitment shift, but results are very sensitive to the movement assumptions, as expected (Figure 18 to 21). Assuming all BET move eastwards at a quarterly rate of 16% stacks practically all the spawning biomass in area A2 (central-onshore equatorial, Figure 7)(Figure 18) and es-

timates more than 80% of the age-0 recruitment occurring in area A1 (offshore equatorial, Figure 7)(Figure 18). Assuming that the movement rates of 16% per quarter apply only to tuna aged 3 to 8 quarters of age still results in a staking of spawning biomass in area A1 (Figure 19) and a shift in the proportion of age-0 recruitment between areas A1 and A2 around the mid-1990s (Figure 19). Results are highly sensitive to assumptions about the catchability (q) and selectivity of the longline fisheries. If q and selectivities are area-specific, q for area A2 is estimated to be two orders of magnitude (Figure 20, top panels), which seems implausible given that the gear is similar between the areas and also the areas are of approximately the same size. If q is mirrored between the areas, but selectivities are area-specific, the model estimates implausible selectivities (not having any size fully selected, therefore modifying the effective catchability) and the fit to the index of the area A2 is degraded (Figure 20, center panels). If q and selectivities are mirrored between the areas then the fit to indices of abundance of areas A1 and A2 are severely degraded (Figure 20 bottom panels) and the model has convergence issues. Lastly, assuming age-dependent eastward movement rate at 16% per quarter for juveniles (aged 3 to 8 quarters) and 5% per quarter diffusion for BET aged 15 quarters and older results in an overall R_{shift} = 1.65 and alternates between A2 and A1 being the main source of age-0 recruits (around 60% for either) around the time of the FAD increase (mid-1990s) (Figure 21), while showing some of the same issues with catchability and selectivity as the previous scenario (q from area A1 estimated to be one order of magnitude larger than q from area A2).

Neither "Alternative 1" nor "Alternative 2" removed the recruitment regime shift with R_{shift} of 2.39 and 2.05 respectively (Figure 22).

For "Alternative 3" (Figure 10) the recruitment shift is less pronounced than in "Alternative 1" and "Alternative 2" with a total R_{shift} of 1.68 for the 3 area model, 1.91 for its area A1 (Figure 10, North of the equator), 1.53 for its area A2 (Figure 10, South of the equator) and 1.18 for its area A3 (Figure 10, central-nearshore equatorial).

3.1.2 Growth misspecification

3.1.2.1 Wrong specification of Richards growth curve

Estimating L1, L2, K and the Richards shape parameter for the area A1 of the "Default" spatial structure results in a smaller estimated Linf (171.12 cm) than the currently used as a fixed parameter in the base case assessment (Linf = 196.34 cm). The smaller Linf has a large impact on the estimated time series of spawning biomass, resulting in a larger stock size and less depleted stock (Figure 23). Estimating growth parameters reduced the recruitment shift from R_{shift} = 2.35 (fixed growth) to 1.3 (estimating growth). Estimating all growth parameters including CVs resulted in a further reduction of the estimated Linf to 166.5 cm and larger estimated CVs (10% for young and 6% for old fish) than those used in the base case (6% and 4% for young and old respectively). A priori the CVs used in the BET base case seem small compared to the more common range of 10%-15% typically seen in most stock assessments, for example those covered during the CAPAM Growth workshop. The meeting report of that workshop states that variation typically increases with age and a constant coefficient of variation (CV) may be the most appropriate assumption in the absence of information, with a value around 10% being commonly observed. Mesocosm studies have indicated a constant CV with mean length, but wild populations are characterized by decreasing variation with mean length, which may be a consequence of length-specific selectivity. So it may be worth considering larger CVs for characterizing BET variability of size at age.

Similar results were obtained by modifying the 2018 BET base case assessment to estimate growth parameters under different uses of CAAL and data weighting of composition data (Table 2): estimating growth resulted in a reduction of the estimated L2, a healthier stock status (Figure 25) and a reduction of the recruitment regime shift from R_{shift} = 1.5 to around 1.2-1.3 when estimating growth (Table 2).

3.1.2.2 Wrong growth curve model

We tried to implement a growth cessation model (Maunder *et al.* 2018) as an alternative to the Richards growth curve used in the base case model. However we found implementation issues in the beta version of SS related to the use of the quarters as years approach used in the BET assessment model. At the time of writing of this draft those issues still remain.

3.1.3 Length-Weight relationship misspecification

The L-W relationships based on longline vs purse-seine caught BET are compared in Figure 26. Purse-seine caught BET tends to weigh less than longline caught BET, with the difference being larger for smaller fish. However that difference is no larger than 6% for smaller fish (Figure), which is lower than the 10% to 15% difference reported by Harley et al. (2005). Consequently the difference in stock assessment model results is small and does not result in changes to the R_{shift} levels.

3.1.4 Model time span

Models starting in 1954 (henceforth referred as historical) result in higher estimated time series of spawning biomass that the base case (Figure 27). They also estimate healthier stock status than the base case with spawning biomass ratios ranging from 0.29 to 0.33 compared to the base case ratio of 0.22 (Table 3). Historical models also have smaller recruitment shifts ranging from R_{shift} = 1.23 to 1.34 compared to 1.5 of the base case. Historical models estimating growth had the lowest R_{shift} = 1.23 to 1.25, even when lambda for the length and age compositions is up weighted to 1 in those model runs. In contrast, the 2018 base case model has lambdas set to 0.05 for the length compositions (Aires-da-Silva et al. 2016) and has an R_{shift} = 1.5, while setting the lambda for length compositions to 1 resulting in an increase of the magnitude of the recruitment shift R_{shift} = 1.97.

Similar to the results reported in section 3.1.2.1 on estimating growth of the shorter time models, the estimated L2 for historical models is smaller (168.8 cm to 172.0 cm) than what is currently used in the base case model (196 cm) (Table 3). Estimating all growth parameters with historical length composition data and up weighting all composition lambdas to 1 results in a R_{shift} = 1.25, a smaller L2 (168.76) and larger CVs of variability at age (CV1 = 10%, CV2=6%) than those used in the base case (CV1 = 6%, CV2=5%)(Table 3). As expected, estimated L2 are negatively correlated with estimated K, so the reduction in L2 for runs with estimated growth results in faster K ranging from 0.19 to 0.25, upwards from the K=0.11 used in the base case assessment (Table 3).

3.1.5 Selectivity misspecification

Including an age-based selectivity to allow for changes in availability by age in combination with the length-based selectivity did not result in improvements on the magnitude of the regime shift and had some estimation issues so it will not be further reported here.

On the other hand, allowing for a right-hand descending limb on the longline selectivity curve, a dome shaped pattern (Figure 28), resulted in larger estimated time series of spawning biomass (Figure 29), as expected, and healthier stock status compared to the base case run, with a reduction in the recruitment shift from R_{shift} = 2.44 for the base case to R_{shift} = 1.33 (Figure 30) for the model with dome shape LL selectivity.

Allowing a dome shape selectivity for longline and estimating growth at the same (all growth parameters except growth CVs) produced similar estimated time series of spawning biomass as the base case run (Figure 29) and smaller R_{shift}= 1.27 (Figure 30). Even if dome shape is estimated in this run for all fisheries, it stays asymptotic for the longline (Figure 28).

3.1.6 Catchability misspecification

Estimating a time-block in catchability (q) for the area A1 of the "Default" spatial structure results in a 5% reduction in q, with almost no effect on any of the model results. Allowing for non proportionality in the relationship between the longline index of abundance and biomass results in an increase of effective catchability as biomass decreases (Figure 31, bottom panel) and therefore diverging spawning biomass trends between the base case and the one allowing non-proportionality in q (Figure 31, top panel).

Using a fixed set of values for a post-1993 block in longline catchability (q) from 0.43 to 1.35 relative to q before 1993 does not markedly change the recruitment shift, with all R_{shift} values remaining above 2.44 and up to R_{shift} = 2.86 when q relative to pre-1993 was fixed at 0.43 (Table 4).

3.1.7 Problems in the longline CPUE standardization

The alternative indices for abundance using different standardizations or data are remarkably similar (Figure 32) so they were not expected to produce markedly different SS model results. Similar to what was reported in the previous section, estimating catchability blocks post 1993 did not result in meaningful changes in relative q after 1993 for any of the alternative indices.

In addition to the block in q, a block in longline selectivities (inflection and 95% width of the logistic curve) was also included for the three alternative indices of abundance but did not result in meaningful changes in overall model results (neither biomass trends, q values, selectivities nor recruitment shifts) from the base case.

4. CONCLUSSIONS

Spatial models of the EPO with no movement do not remove the recruitment regime shift. This is in contrast with what was found by Aires-da-Silva and Maunder (2010) and Valero *et al.* (2018). Here we run a very similar spatial configuration ("Alternative 3") to the one used by Aires-da-Silva and Maunder (2010) and although the recruitment shift is less pronounced in that spatial configuration than in other in the alternatives evaluated here, the recruitment shift still remains. Valero *et al.* (2018) used alternative subdivisions for the whole EPO to run different ASPM models that only marginally reduced the recruitment shift depending on configurations, but the focus of their work was on doing a separate analyses of the Central equatorial area that had been identified previously Aires-da-Silva and Maunder (2010) as the source of the recruitment shift. At the time of the Valero *et al.* (2018) work, data was available only for the Central area, so alternative SS model runs were not able to be carried out for the rest of the EPO. Based on work presented here, the source of the recruitment shift seems to be in the dynamics of the area to the west of the Central area used in Aires-da-Silva and Maunder (2010) and Valero *et al.* (2018).

Movement at 16% per quarter seems too high, even if just for juveniles. Including East-West diffusion of adults removes the recruitment shift; however we do not know what reasonable movement rates are for adult BET and results are highly sensible to assumed movement general patterns and rates.

Alternative movement scenarios could be explored. In addition, Pacific-wide assessments with the Secretariat of the Pacific Community (SPC) should be explored, or at least including some of the adjacent assessment model boxes from the central Pacific Ocean. Some of this work has been performed by Valero *et al.* 2019.

Estimating growth reduces markedly the recruitment shift; it also estimates faster growth K, smaller lengths for the older fish and larger CVs of growth. This results in larger estimated time series of biomass and healthier stock status than the base case.

Historical models starting in 1954 rather than 1975 also reduce the recruitment regime shift, although not to the degree that estimating growth does. Historical models also produced similar estimated trends

to the shorter base case model, although with larger biomass series and healthier stock status.

Using dome shape selectivities for all gears also reduced the recruitment shift and produced similar results as runs with estimated growth, with larger biomass series and healthier stock status.

Using time blocks for catchability and selectivity of the longline fisheries did not produced markedly different results from the base case.

A better understanding of BET spatial structure, spatial dynamics but also basic life history such as growth, L-W relationships and use of available historical data is important to improve the EPO BET stock assessments and also to implement useful operating models for ongoing BET MSE work.

5. REFERENCES

Aires-da-Silva A. and M. Maunder, 2010. An evaluation of spatial structure in the stock assessment of bigeye tuna in the eastern Pacific Ocean. Inter-Amer. Trop. Tuna Comm. Document BET-01-02b. External review of IATTC bigeye tuna assessment. La Jolla, California, USA. 3-7 May 2010.

Aires-da-Silva A. and M. Maunder. 2014. Status of bigeye tuna in the eastern Pacific Ocean in 2013 and outlook for the future.

Aires-da-Silva, A., M. N. Maunder, and P. K. Tomlinson. 2010. An investigation of the trend in the estimated recruitment for bigeye tuna in the eastern Pacific Ocean. Document BET-01-06. Inter-Amer. Trop. Tuna Comm. Document BET-01-02b. External review of IATTC bigeye tuna assessment. La Jolla, California, USA. 3-7 May 2010.

Aires-da Silva, A. M., Maunder, M. N., Schaefer, K. M., and Fuller, D. W. 2015. Improved growth estimates from integrated analysis of direct aging and tag-recapture data: An illustration with bigeye tuna (*Thunnus obesus*) of the eastern Pacific Ocean with implications for management. Fisheries Research, 163: 119-126.

Aires-da-Silva, A., Minte-Vera, C., and M.N. Maunder. 2017. Status of bigeye tuna in the eastern Pacific Ocean in 2016 and outlook for the future. Inter-Amer. Trop. Tuna Comm. SAC-08-04a.

Anonymous. 2019. Growth used in the EPO bigeye tuna assessment. Review of the stock assessment of bigeye tuna in the eastern Pacific Ocean. La Jolla, California (USA), 11-15 March 2019.

Cope, J.M., Punt, A.E., 2011. Reconciling stock assessment and management scales under conditions of spatially varying catch histories. Fish. Res. 107, 22–38.

Fonteneau, A., and Ariz, J. 2008. An overview of 10 years of IATTC bigeye stock assessments in the Eastern Pacific Ocean. In 'The 9th Stock assessment review meeting, La Jolla, 12–16 May 2008'. (Inter-American Tropical Tuna Commission: La Jolla, San Diego, CA.)

Fonteneau, A., Chassot, E., Bodin, N., 2013. Global spatio-temporal patterns in tropical tuna purse seine fisheries on drifting fish aggregating devices (DFADs): taking a historical perspective to inform current challenges. Aquat. Living Resour. 26,37–48.

Francis, R. 2011. Data weighting in statistical fisheries stock assessment models. Can J Fish Aquat Sci. 68: 1124-1138.

Harley S. J., Maunder, M. N., Deriso, R. B. 2005. Assessment of bigeye tuna (*Thunnus obesus*) in the eastern Pacific Ocean. Col. Vol. Sci. Pap. ICCAT, 57(2): 218-241

Hurtado-Ferro, F., Punt, A.E. and Hill, K.T. 2014. Use of multiple selectivity patterns as a proxy for spatial structure. Fisheries Research 158, 102–115.

Kume, S., Joseph, J. 1966. Size composition, growth and sexual maturity of Bigeye Tuna, *Thunnus obesus* (Lowe), from the Japanese longline fishery in the eastern Pacific Ocean. Inter-Amer. Trop. Tuna Comm. Bull. 11:45–99.

Lennert-Cody, C., M.N. Maunder, and A. Aires-da-Silva. 2010. Preliminary analysis of spatial-temporal pattern in bigeye tuna length-frequency distributions and catch-per-unit-effort trends. BET-01-02. External review of IATTC bigeye tuna assessment, La Jolla, California, USA, 3-7 May, 2010.

Lennert-Cody, C.E., Mauder, M.N., Aires-da-Silva, A., Minami, M. 2013. Defining population spatial units: Simultaneous analysis of frequency distributions and time series. Fis. Res/ 139: 85-92. http://dx.doi.org/10.1016/j.fishres.2012.10.001

Maunder, M.N., and Piner, K.R. 2015. Contemporary fisheries stock assessment: many issues still remain. ICES Journal of Marine Science (2015), 72(1), 7–18. doi:10.1093/icesjms/fsu015.

Maunder, M.N., Aires-da-Silva, A. and Lennert-Cody, C.E. Summary of issues in the Eastern Pacific Ocean Bigeye Tuna assessment. 2010. Inter-Amer. Trop. Tuna Comm. Document BET-01-01. External review of IATTC bigeye tuna assessment. La Jolla, California, USA. 3-7 May 2010.

Maunder, M. N., Aires-da-Silva, A., Minte-Vera, C and Valero, J. L. 2016. Current and future research on management strategy evaluation (MSE) for tunas and related species in the Eastern Pacific Ocean. Inter-Amer. Trop. Tuna Comm., 7th Scient. Adv. Com. Meeting. SAC-07.

Maunder, M.N., Thorson, J.T., Lee, H.H., Kai, M., Chang, S.K., Kitakado, T., Albertsen, C.M., Lennert-Cody, C.E., Aires-da-Silva, A.M., Piner, K.R. 2017. The need for spatial-temporal modeling of catch-per-unit-effort data when used to derive indices of relative abundance to include in stock assessment models. Inter-Amer. Trop. Tuna Comm., 8th Scient. Adv. Com. Meeting. SAC-08-05d.

Maunder, M.N., Deriso, R.B., Schaefer, K.M., Fuller, D.W., Aires-da-Silva, A.M., Minte‑Vera, C.V., Campana, S.E. 2018. The growth cessation model: a growth model for species showing a near cessation in growth with application to bigeye tuna (*Thunnus obesus*). Marine Biology (2018) 165:76.

Methot, R. D. 2005. Technical description of the Stock Synthesis II assessment program. NOAA Fisheries. http://www.sefsc.noaa.gov/sedar/download/S16_AW_04.pdf

Methot, R.D., and Wetzel, C.R. 2013. Stock Synthesis: A biological and statistical framework for fish stock assessment and fishery management. Fish Res. 142: 86-99.

Minte-Vera, C. V., Maunder, M. N., Aires-da-Silva, A. M., Satoh, K., Uosaki, K. Get the biology right, or use size-composition data at your own risk. 2017. Fisheries research. 192: 114-125.

Minte-Vera *et al.* 2019. A spatial structure for bigeye tuna in the eastern Pacific Ocean. Review of the stock assessment of bigeye tuna in the eastern Pacific Ocean. La Jolla, California (USA), 11-15 March 2019.

Miyabe, N., Bayliff, W.H., 1998. A review of information on the biology, fisheries, and stock assessment of bigeye tuna, *Thunnus obesus*, in the Pacific Ocean. Inter-Am. Trop. Tuna Comm. Spec. Rep. 9, 129–170.

Miyake, M.P., Miyabe, N., Nakano, H., 2004. Historical trends of tuna catches in the world. FAO Fish. Tech. Pap. 467, 74 pp.

Nakamura, E.L. and J.H. Uchiyama. 1966. Length-weight relations of Pacific tunas. In Manar, T.A. (editor), Proc., Governor's [Hawaii] Conf. Cent. Pacif. Fish. Resources: 197-201.

Schaefer, K. M., D. W. Fuller. 2002. Movements, behavior, and habitat selection of bigeye tuna (*Thunnus obesus*) in the eastern equatorial Pacific, ascertained through archival tags. Fish. Bull. 100: 765-788.

Schaefer, K.M. 2009. Stock structure of bigeye, yellowfin, and skipjack tunas in the eastern Pacific Ocean. Inter-Amer. Trop. Tuna Comm., Stock Assess. Rep. 9. 203-221

Schaefer, K.M. and D.W. Fuller. 2009. Horizontal movements of bigeye tuna (*Thunnus obesus*) in the eastern Pacific Ocean, as determined from conventional and archival tagging experiments initiated during 2000-2005. IATTC Bulletin, Vol. 24(2).

Schaefer, K., Fuller, D., Hampton, J., Caillot, S., Leroy, B., and Itano, D. 2015. Movements, dispersion, and mixing of bigeye tuna (*Thunnus obesus*) tagged and released in the equatorial Central Pacific Ocean, with conventional and archival tags. Fisheries Research, 161:336-355.

Skillman, A., R., Boggs, C. H., and Pooley, S. 1993. Fishery interaction between the tuna longline and other pelagic fisheries in Hawaii. NOAA Technical Memorandum NMFS 189.

Valero, J. L., Aires-da-Silva, A. and Maunder, M. N. 2018. Exploratory spatial stock assessment of Bigeye tuna (*Thunnus obesus*) in the EPO. SAC-09

Valero *et al.* 2019. Spatial stock assessment model options for BET in the EPO and beyond. Review of the stock assessment of bigeye tuna in the eastern Pacific Ocean. La Jolla, California (USA), 11-15 March 2019.

Valero, J. L. 2019. Conversion of BET 2017 base case assessment from Stock Synthesis version 3.23b to 3.3. Review of the stock assessment of bigeye tuna in the eastern Pacific Ocean. La Jolla, California (USA), 11-15 March 2019.

Watters, G.M. 1999. Geographical distributions of effort and catches of tunas by purse-seine vessels in the eastern Pacific Ocean during 1965-1998. IATTC Data Report 10.

TABLES

TABLE 1. Overview of differences between current BET stock assessment model configurations and the exploratory alternative models implemented to investigate potential causes of the estimated recruitment regime-shift.

CURRENT BASE CASE	EXPLORATORY MODELS
SS version 3.23b	**SS version 3.3.12**
Years as Quarters approach	Years as Quarters approach
–Years 1975 to 2017 as Quarters 1 to 168	–Years 1975 to 2018 as Quarters 1 to 172
Max age 40 quarters (10 years)	Max age 40 quarters (10 years)
2-sex model	2-sex model
Growth: fixed Richards function	Growth: Richards, Growth Cessation, fixed or estimated
Fixed age/sex specific natural mortality	Fixed age/sex specific natural mortality
Steepness h=1	Steepness *h*=1
Lambda length comps = 0.05	**Lambda length comps = 0.05, 1, Francis**
Length bins = 2 cm	**Length bins = 10 cm**
1 Area	**1 to 4 Areas**
27 fleets	**4 to 20 fleets**
245 parameters	**230 to 800 parameters**
3 to 8 hours run time	**0.2 to 3 hours run time**

TABLE 2. Alternative BET SS model runs estimating or fixing growth. "Base" is the 2018 base case BET stock assessment, "Base_estG" is identical to the "Base" but estimating L1, L2, K and the shape parameter of the Richards growth function, "Base_estG_CAAL" uses Conditional-Age-At-Length with a lambda of 1, ""Base_estG_CAAL_lambda1" uses lambda 1 for all age and length composition data.

	Base	Base_estG	Base_estG_CAAL	Base_estG_CAAL_lambda1
TOTAL_like	126.1	102.8	386.7	2517.8
Survey_like	-400.8	-399.5	-398.1	-359.3
Length_comp_like	580.1	558.3	568.7	2594.8
Age_comp_like	0	0	271.6	312.2
Bratio_172	0.22	0.34	0.32	0.32
F_172	1.22	0.75	0.82	0.45
SPRratio_172	1.08	0.89	0.94	0.69
L_at_Amin_Fem_GP_1	29.23	31.97	27.23	30.43
L_at_Amax_Fem_GP_1	196.34	172.90	176.50	172.05
VonBert_K_Fem_GP_1	0.11	0.21	0.17	0.19
Richards_Fem_GP_1	0.23	-1.10	-0.30	-0.76
SD_young_Fem_GP_1	1.83	1.83	1.83	1.83
SD_old_Fem_GP_1	8.88	8.88	8.88	8.88
R_{shift}	1.50	1.22	1.35	1.27

TABLE 3. Alternative BET SS model runs starting in 1975 ("Base") or 1954 ("HistC"), fitting to historical longline length compositions ("LF"), estimating ("estG") or fixing growth, and estimating CVs ("CV") of growth or fixing CVs. "Base" is the 2018 base case BET stock assessment. Combinations estimating growth ("estG") use lambda of 1 for all composition data. Table coloring is just to highlight differences.

	Base	HistC	HistC_LF	HistC_estG	HistC_LF_estG	HistC_LF_estG_CV
TOTAL_like	126.13	85.94	87.68	2473.72	2481.20	2432.25
Survey_like	-400.84	-397.74	-397.75	-358.93	-358.94	-359.87
Length_comp_like	580.15	581.55	583.18	2592.96	2599.74	2550.03
Age_comp_like	0.00	0.00	0.00	312.35	312.51	295.74
Bratio_LastYr	0.22	0.29	0.29	0.33	0.33	0.33
F_LastYr	1.22	1.02	1.03	0.43	0.44	0.45
SPRratio_LastYr	1.08	1.00	1.00	0.67	0.67	0.69
L_at_Amin	29.23	29.23	29.23	30.44	30.44	35.16
L_at_Amax	196.34	196.34	196.34	172.01	171.73	168.76
VonBert_K	0.11	0.11	0.11	0.19	0.20	0.25
Richards	0.23	0.23	0.23	-0.77	-0.77	-1.64
SD_young	1.83	1.83	1.83	1.83	1.83	3.68
SD_old	8.88	8.88	8.88	8.88	8.88	10.53
CV_young	0.06	0.06	0.06	0.06	0.06	0.10
CV_old	0.05	0.05	0.05	0.05	0.05	0.06
R_{shift}	1.50	1.34	1.34	1.23	1.23	1.25

Table 4. Recruitment shift (R_{shiftI}) estimated for SS runs for the area A1 of the "Default" spatial structure with a time block in 1993 for catchability (q) of the longline index for a range of fixed q. "q relative to pre-1993" is the catchability of the block after 1993 relative to the catchability pre-1993.

q relative to pre-1993	R_{shift}
0.43	2.86
0.88	2.61
1	2.44
1.15	2.56
1.35	2.53

FIGURES

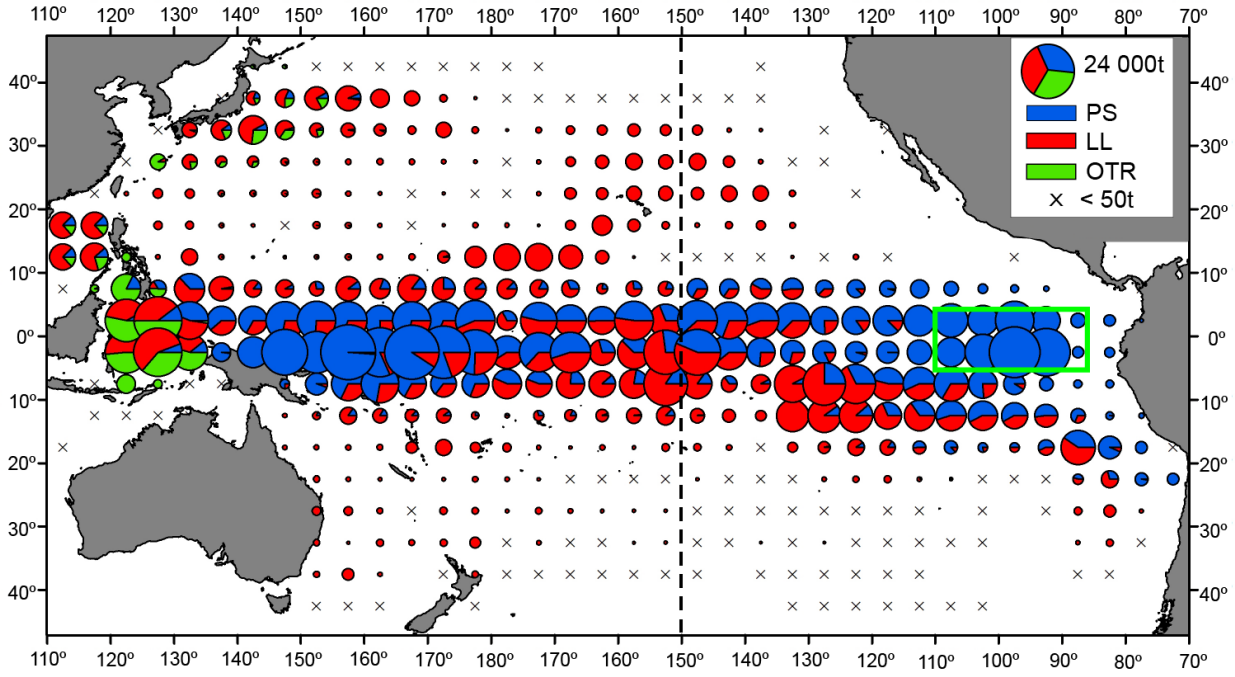

FIGURE 1. Distribution of the catches of bigeye tuna in the Pacific Ocean, by 5° x 5° area and gear type, 2008-2012. The sizes of the circles are proportional to the catch. The vertical dashed line at 150°W marks the western boundary of the eastern Pacific Ocean (EPO). The green rectangle represents the Central area used Valero et al. 2018. PS: purse seine; LL: longline; OTR: other gears.

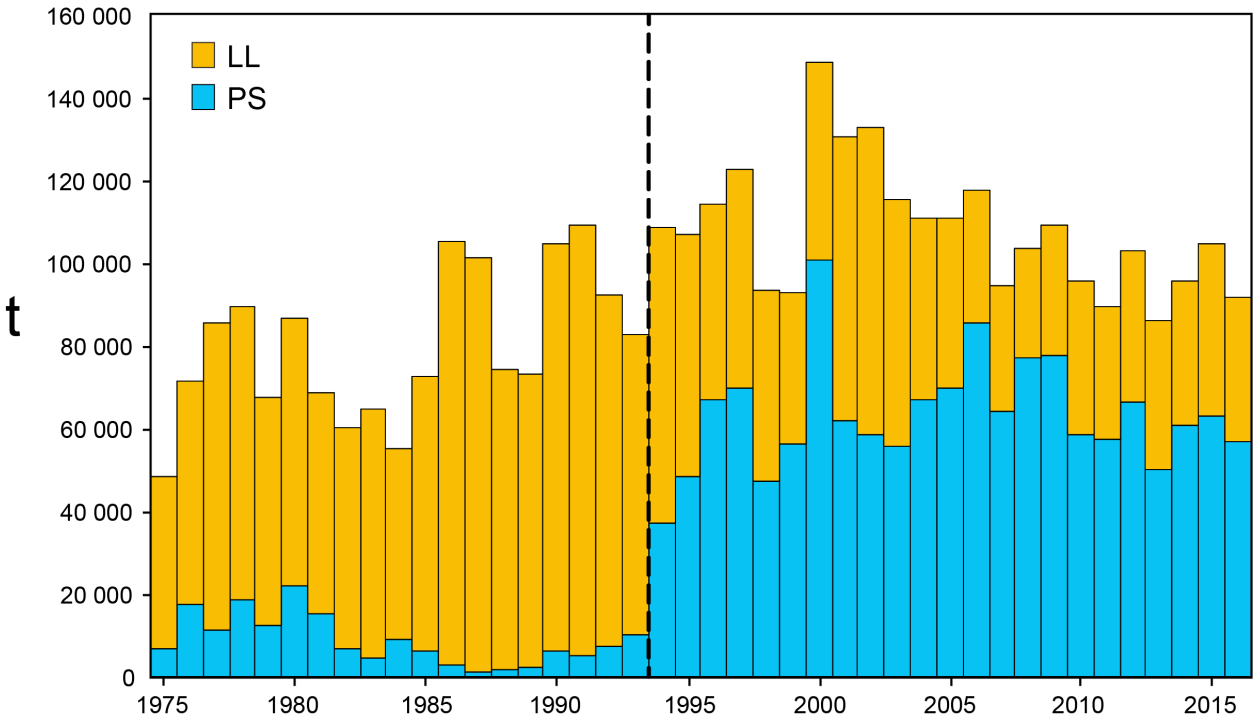

FIGURE 2. Annual catches of bigeye tuna in the eastern Pacific Ocean, by gear, 1975-2016, showing the sudden change (dashed vertical line) resulting from the introduction of fish-aggregating devices (FADs) in the early 1990s. PS: purse seine; LL: longline.

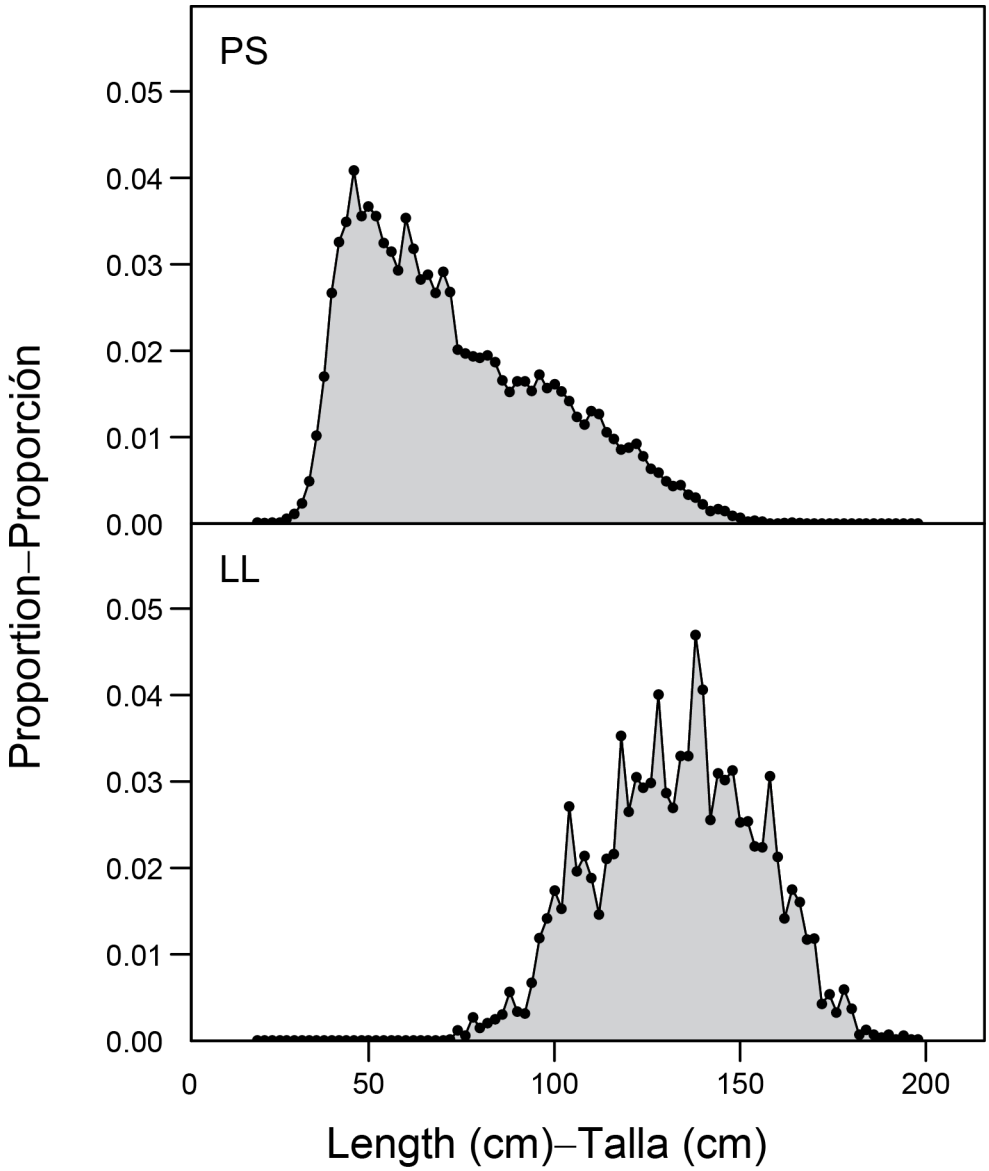

FIGURE 3. Length compositions of bigeye tuna caught in the Central area, by fleet, 1975-2016. PS: purse seine; LL: longline.

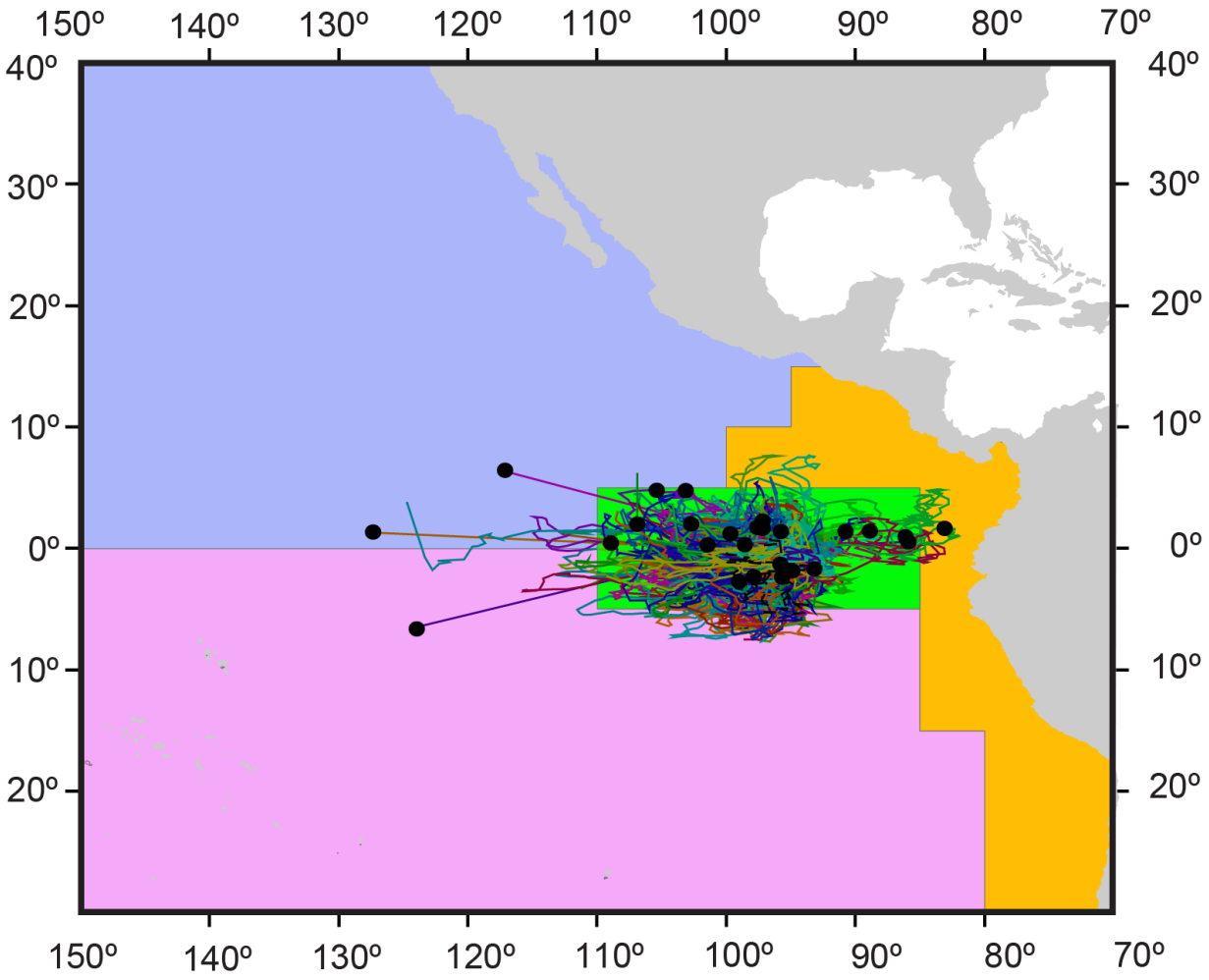

FIGURE 4. Movement paths of bigeye tuna at liberty for 30 days or longer, inferred from archival tagging data from 2000-2006 (Schaefer and Fuller 2009).

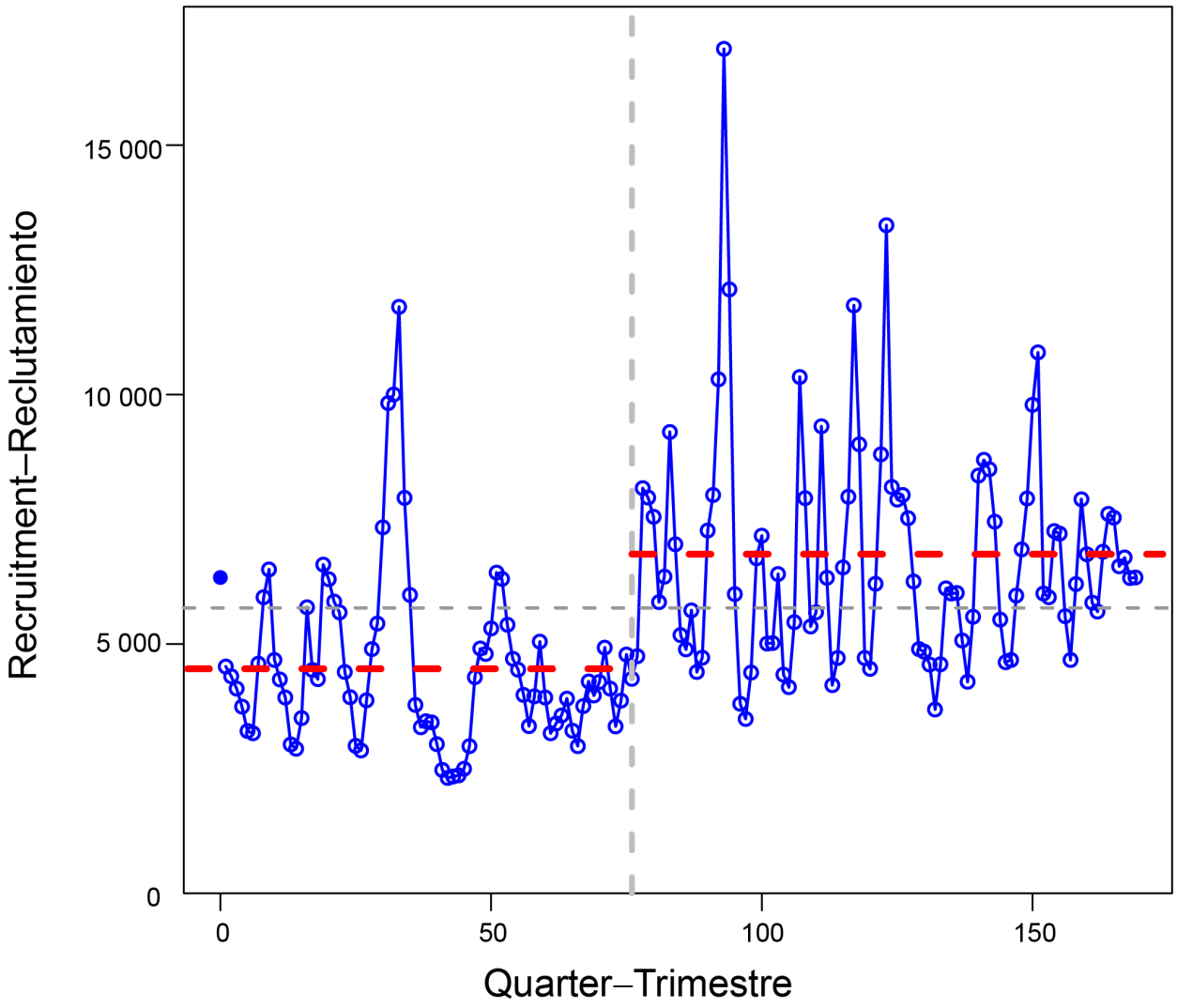

FIGURE 5. Time series of estimated recruitment, in thousands of fish, during 1975-2016, showing apparent two-regime pattern before and after 1995.

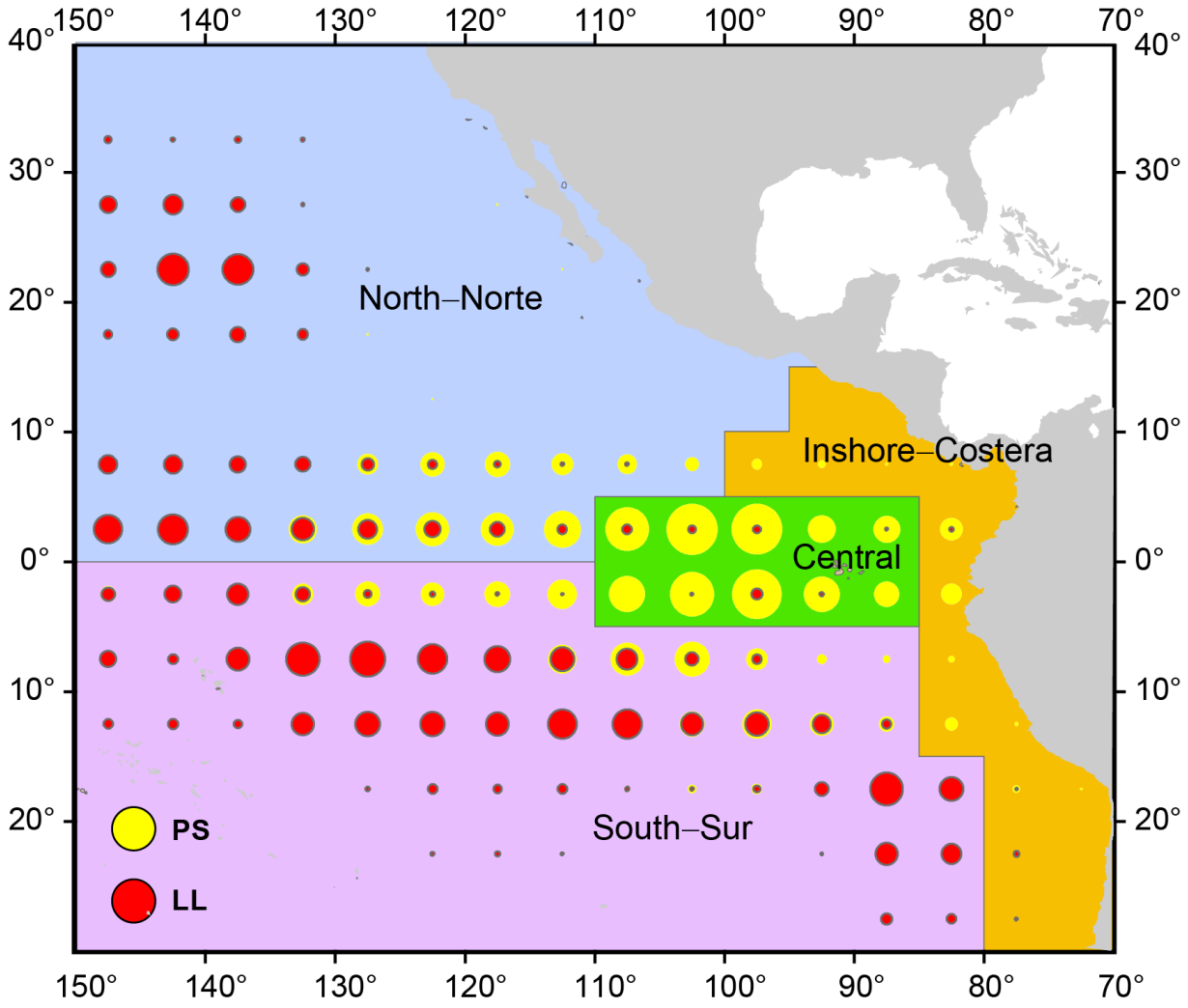

FIGURE 6. Spatial distribution of the catches of bigeye tuna in the eastern Pacific Ocean, 2000-2006, by gear and sub-stock (North, South, Central, and Inshore). The sizes of the circles are proportional to the catch (from Aires-da-Silva and Maunder 2010). PS: purse seine; LL: longline.

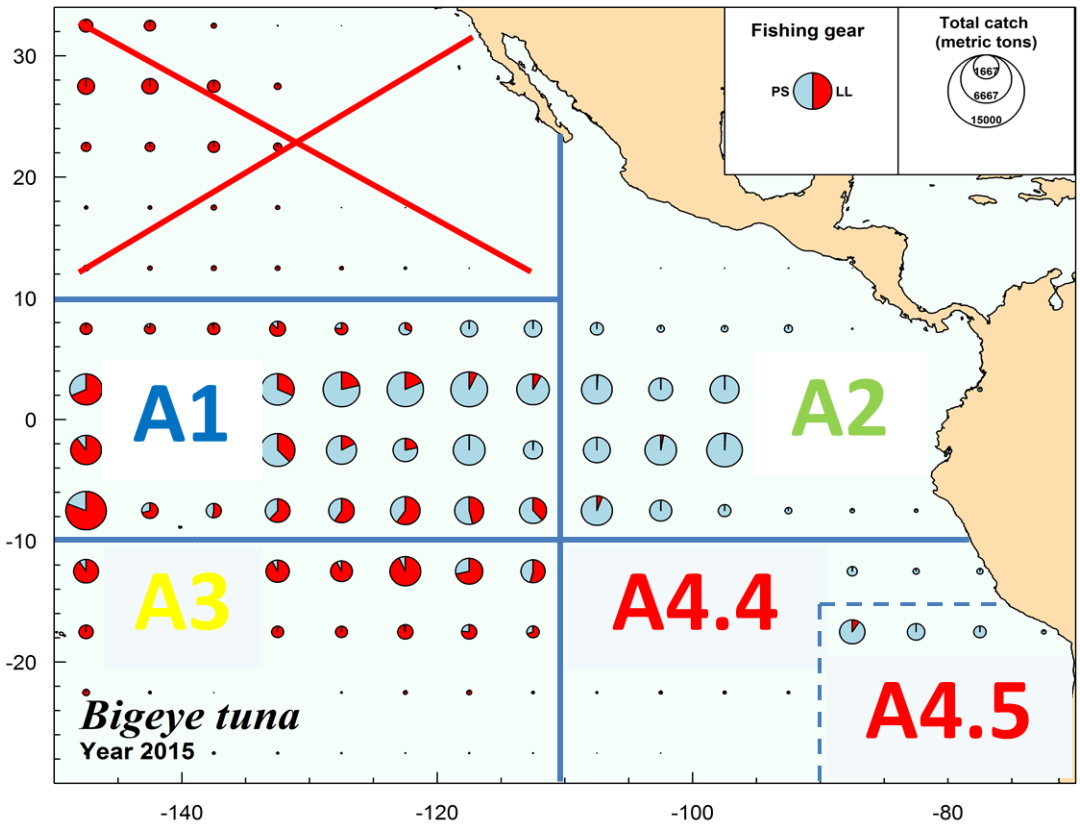

Figure 7. "Default" spatial structure configuration for BET in the EPO descrcibed in Minte-Vera *et al.* (2019).

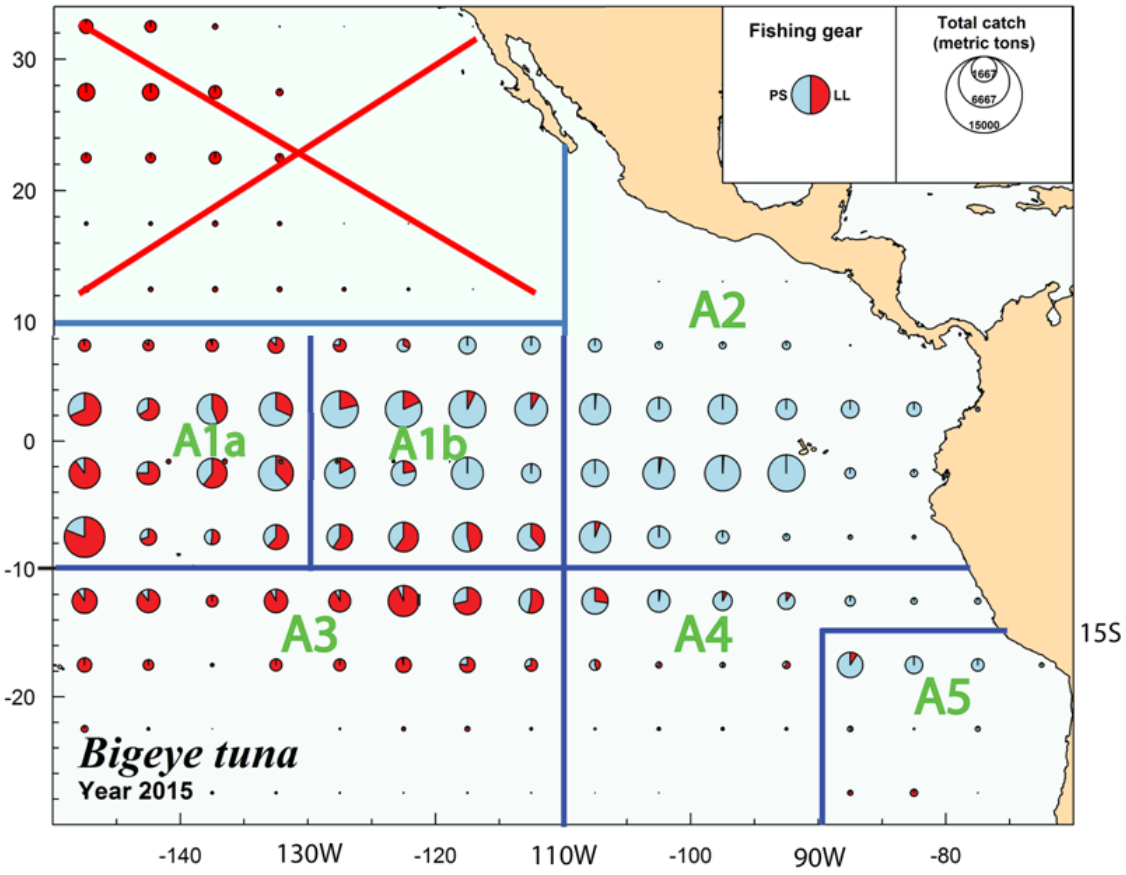

Figure 8. "Alternative 1" spatial structure configuration for BET in the EPO, further dividing the offshore equatorial area at 130W.

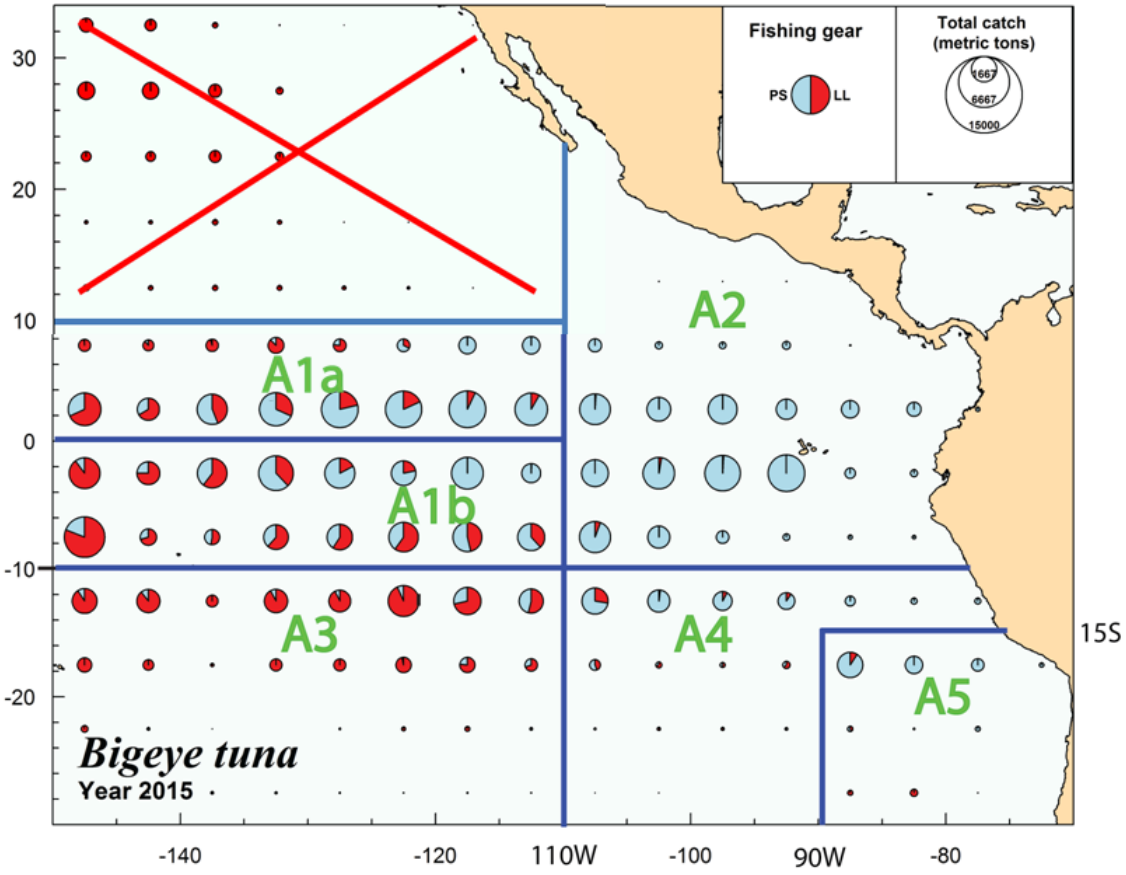

Figure 9. "Alternative 2" spatial structure configuration for BET in the EPO, further dividing the offshore equatorial area at the equator.

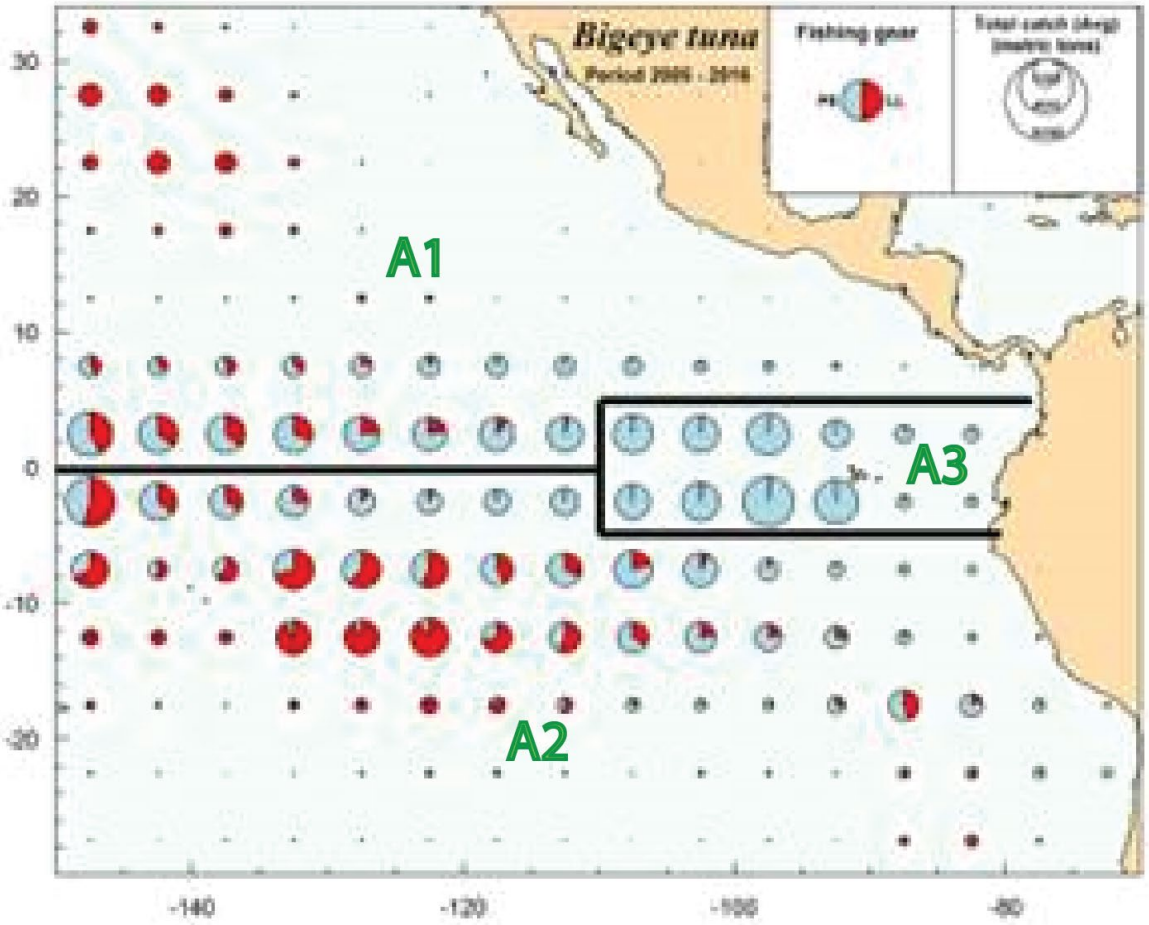

Figure 10. "Alternative 3" spatial structure configuration for BET in the EPO, following the spatial structure used in Aires-da-Silva and Maunder (2010), except the coastal component has been merged with the other areas.

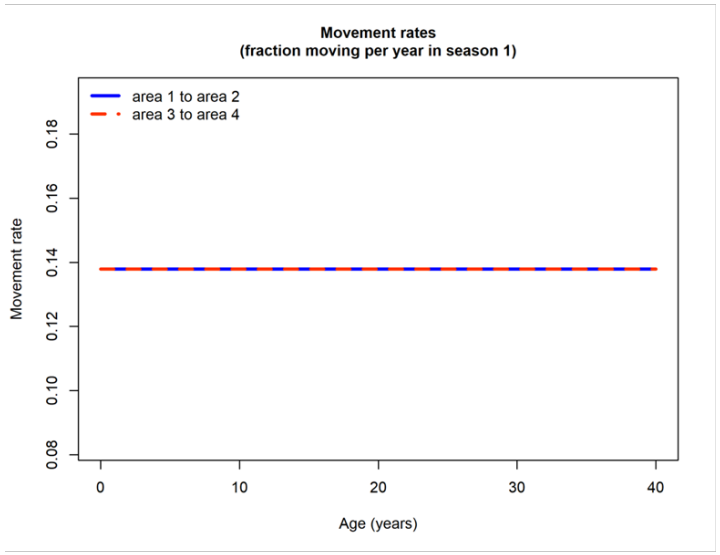

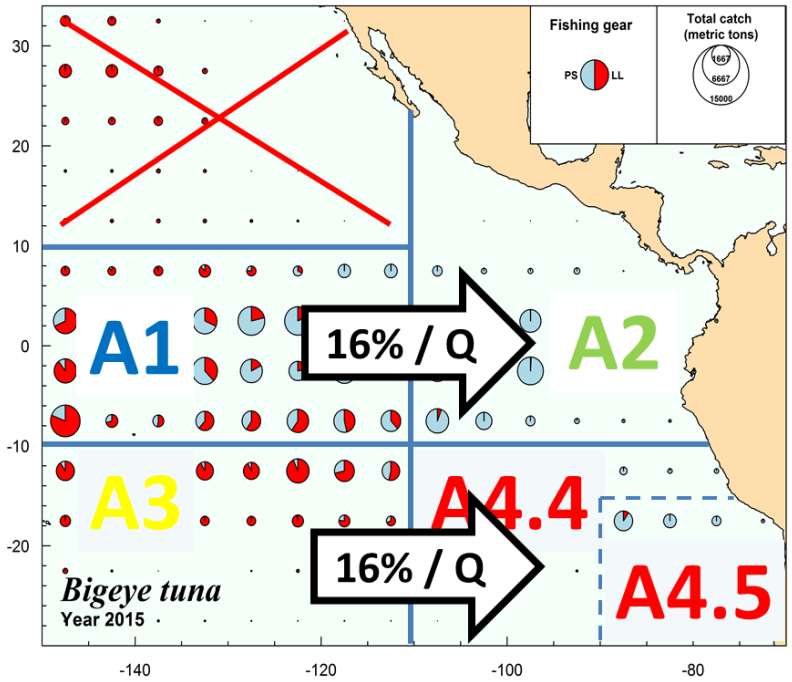

Figure 11. Movement scenario for the "Default" BET spatial structure: age-invariant eastward movement at 16% per quarter.

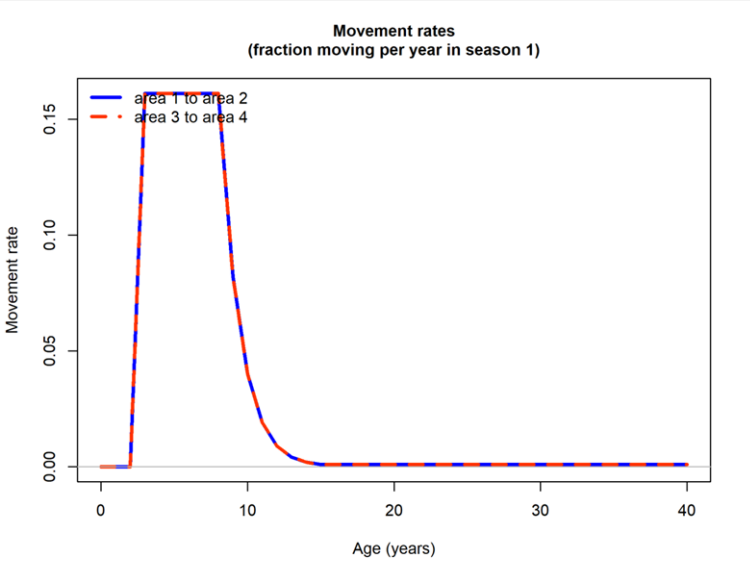

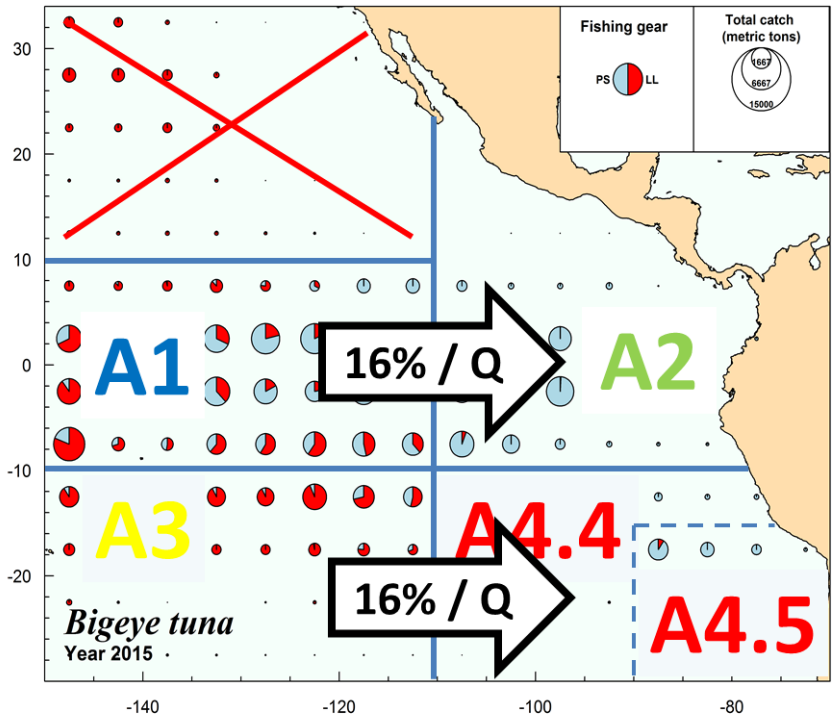

Figure 12. Movement scenario for the "Default" BET spatial structure: eastward movement at 16% per quarter only for juveniles (aged 3 to 8 quarters), no movement for the other ages.

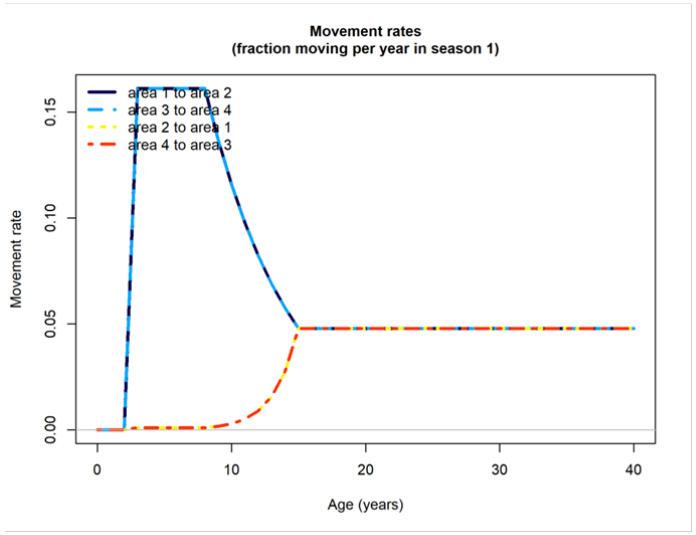

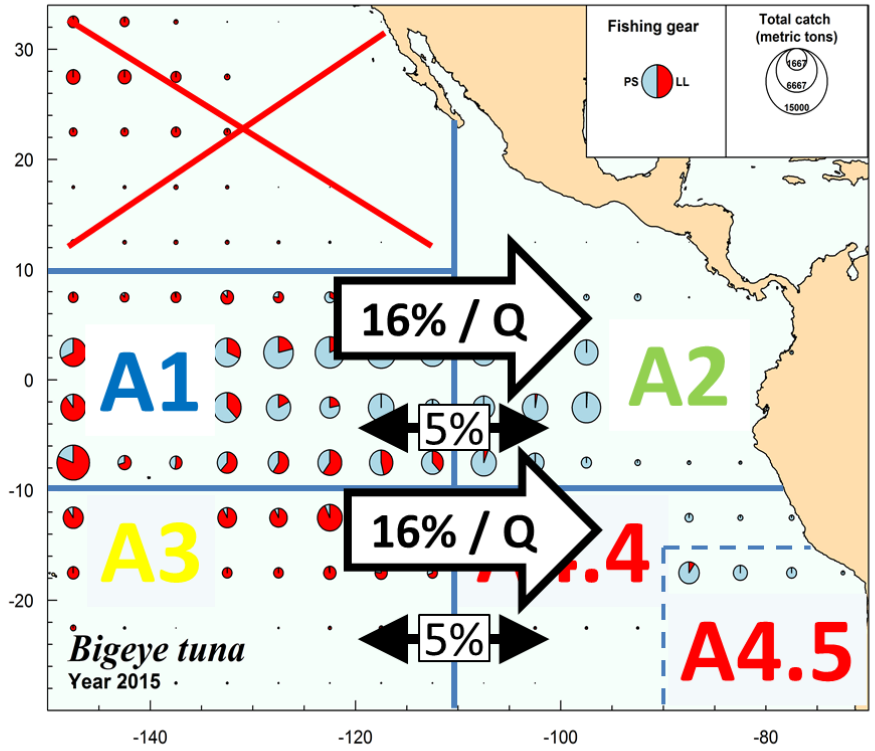

Figure 13. Movement scenario for the "Default" BET spatial structure: eastward movement rate at 16% per quarter for juveniles (aged 3 to 8 quarters) and 5% per quarter E-W diffusion for BET aged 15 quarters and older.

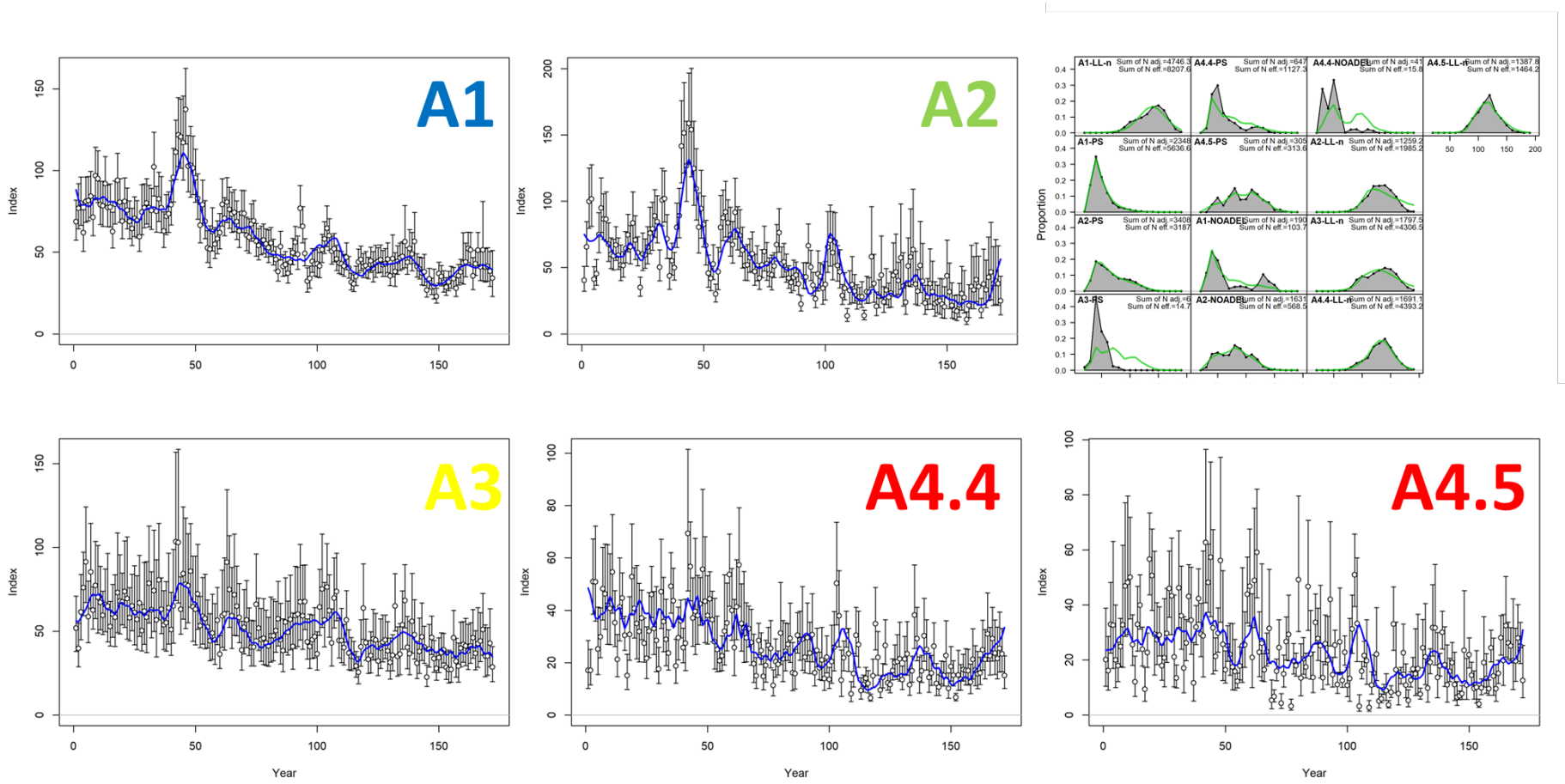

Figure 14. Model fits to the indices of abundance and time-aggregated length composition data for the "Default" spatial configuration with no movement.

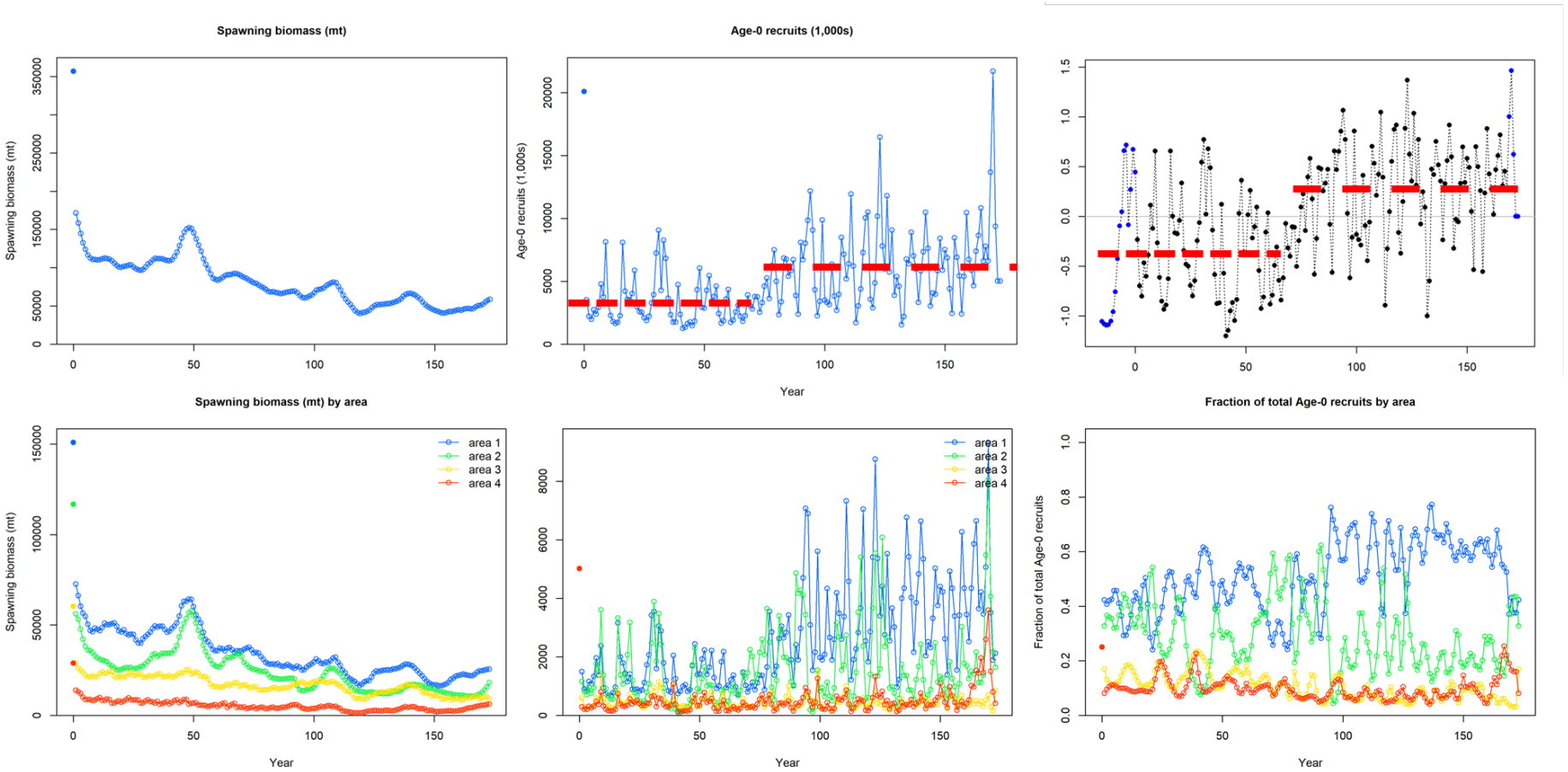

Figure 15. Estimated time-series for the "Default" spatial configuration with no movement. Top panels from the left: Total Spawning biomass, Total age-0 recruits, Total recruitment deviates. Red dashed line highlights the regime shift in the mid-1990s. Bottom panels from the left: Area specific time series of Spawning biomass, Age-0 recruitment and Fraction of total age-0 recruits.

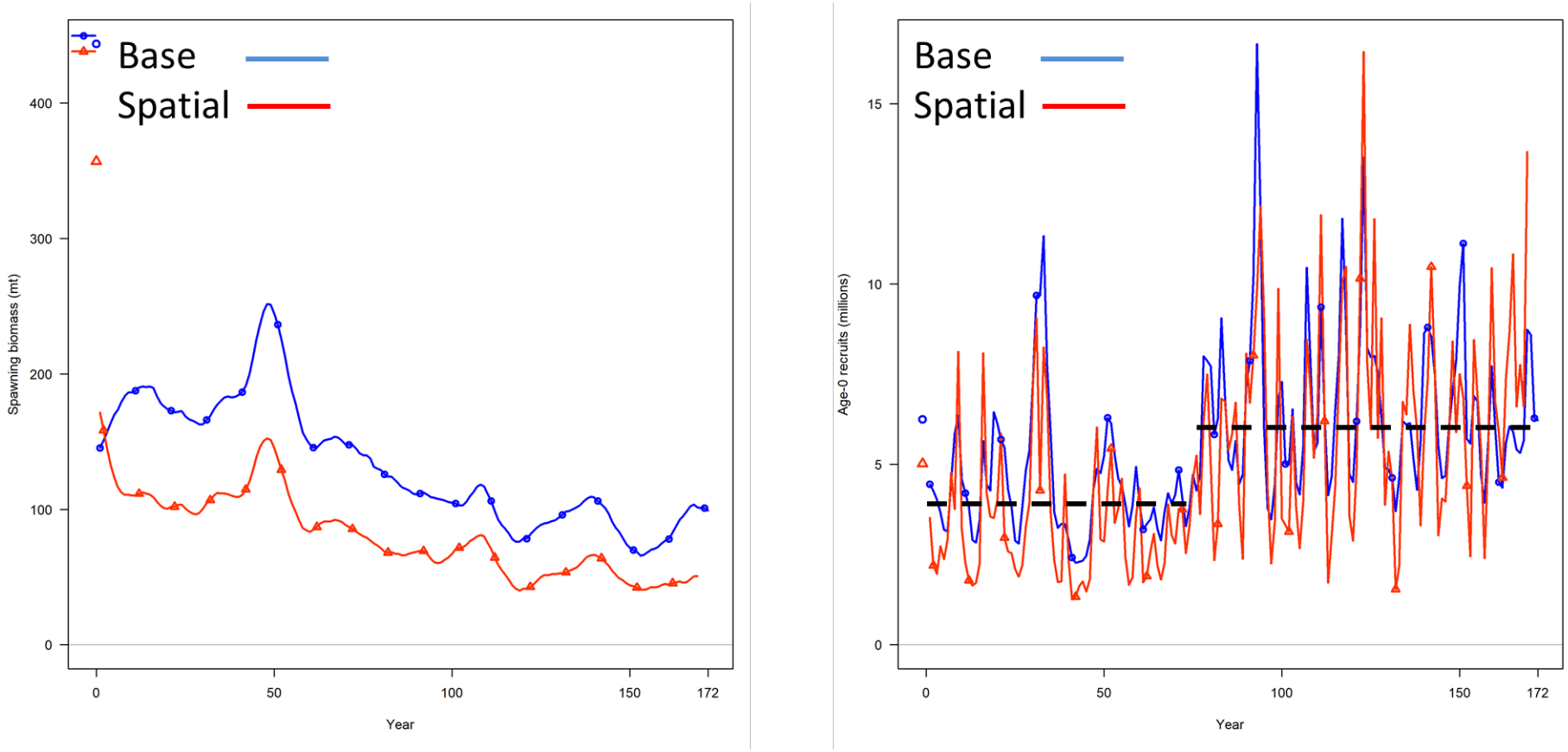

Figure 16. Left panel: time series of estimated Spawning biomass for the BET base case assessment (blue line) and a spatial model with no movement under the "Default" spatial structure assumption. Right panel: time series of estimated age-0 recruits, the dashed lines correspond to the change in recruitment levels estimated in the mid-1990s.

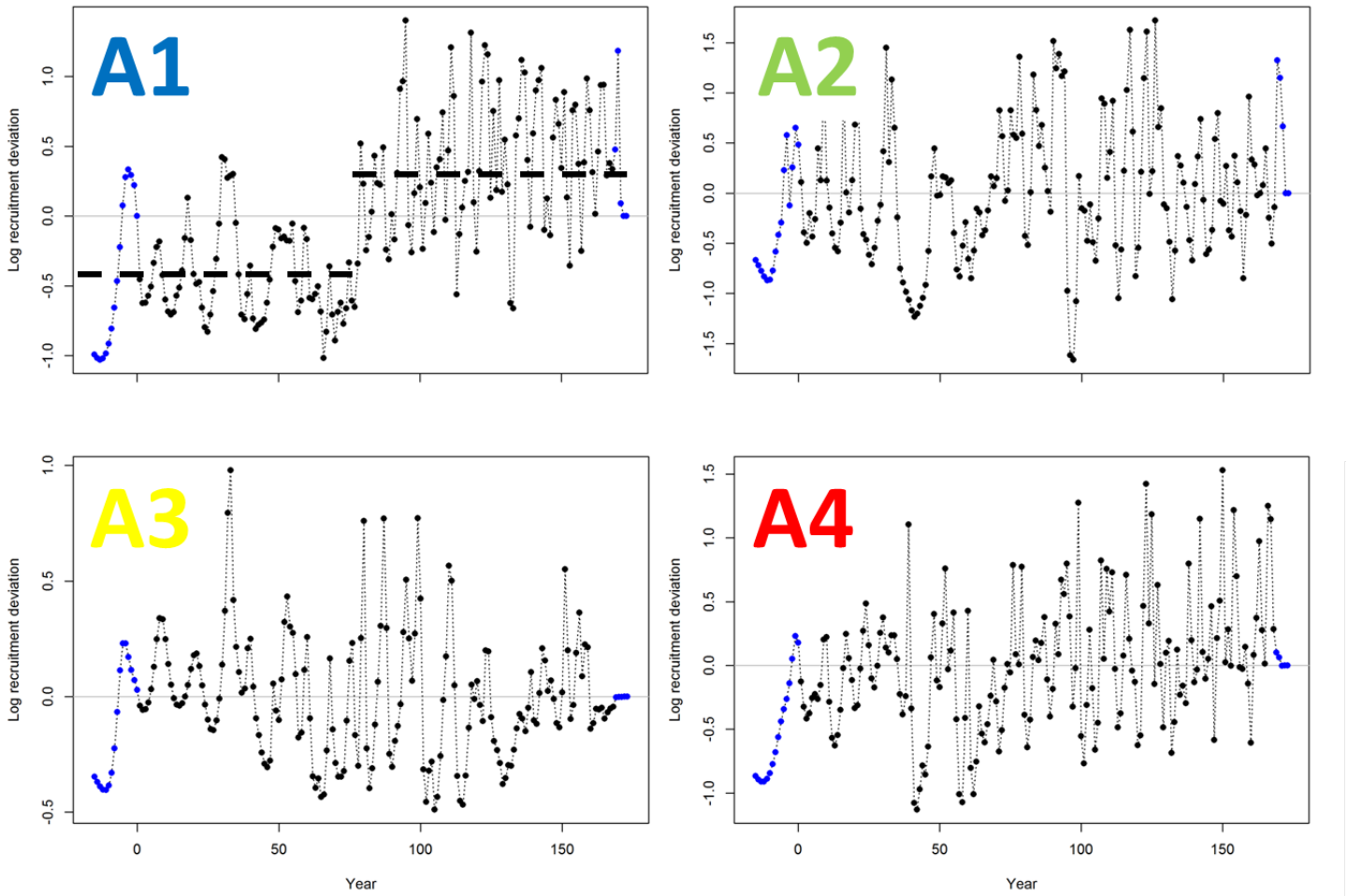

Figure 17. Area-specific time series of recruitment deviations for the four independent area models of the "Default" spatial structure.

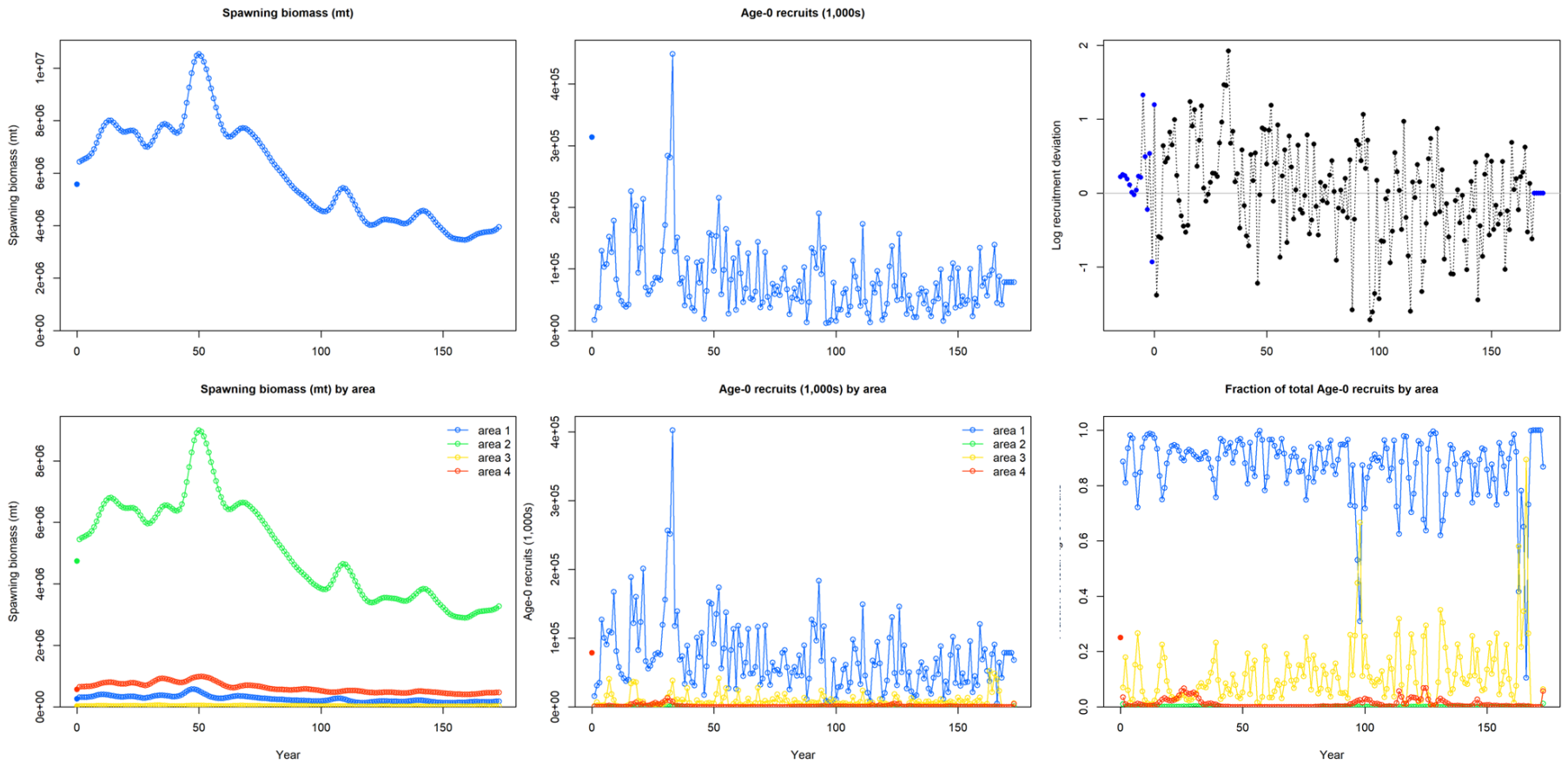

Figure 18. Estimated time-series for the "Default" spatial configuration with age-independent movement at 16% per quarter. Top panels from the left: Total Spawning biomass, Total age-0 recruits, Total recruitment deviates. Bottom panels from the left: Area specific time series of Spawning biomass, Age-0 recruitment and Fraction of total age-0 recruits.

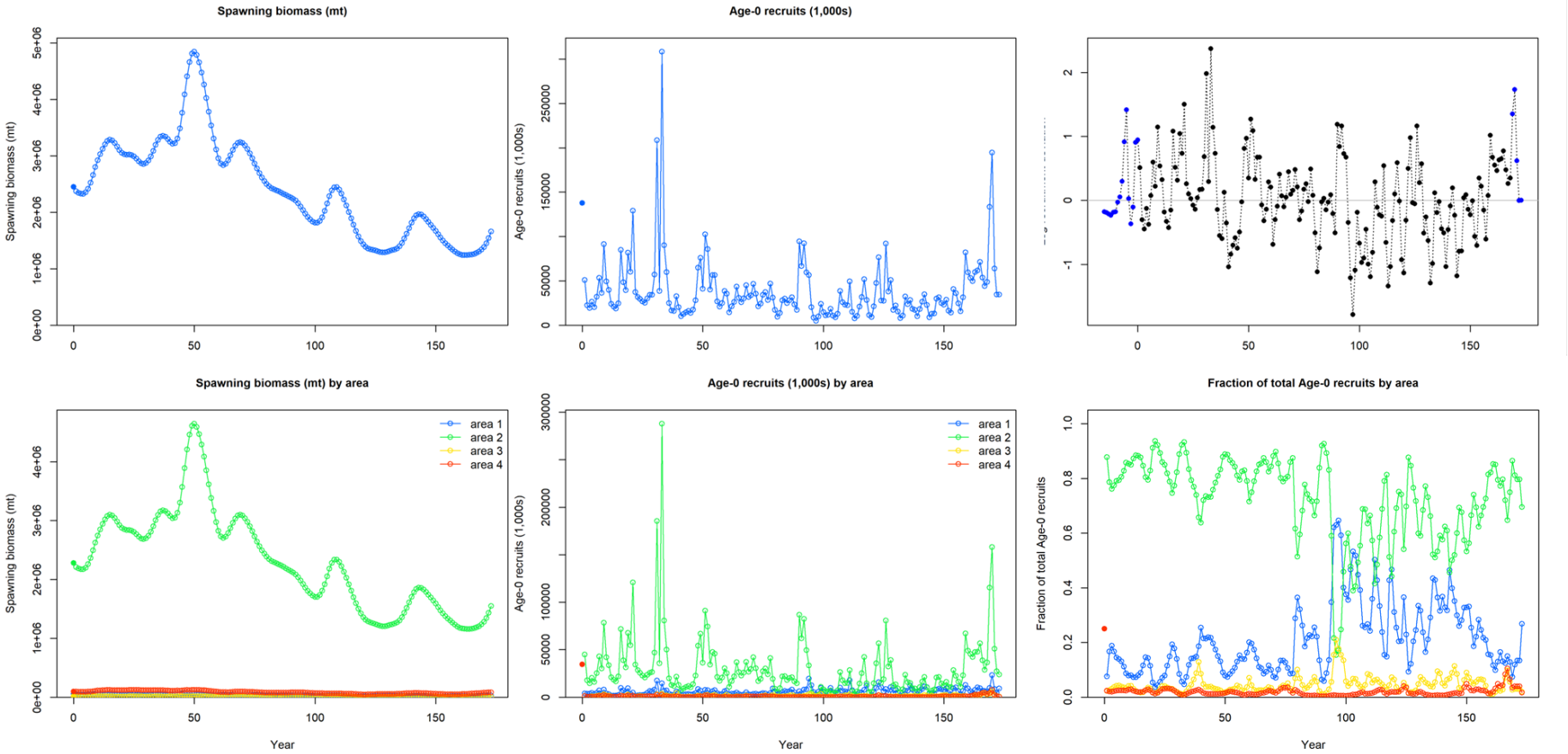

Figure 19. Estimated time-series for the "Default" spatial configuration with age-dependent eastward movement rate at 16% per quarter for only juveniles (aged 3 to 8 quarters), no movement for the other ages. Top panels from the left: Total Spawning biomass, Total age-0 recruits, Total recruitment deviates. Bottom panels from the left: Area specific time series of Spawning biomass, Age-0 recruitment and Fraction of total age-0 recruits.

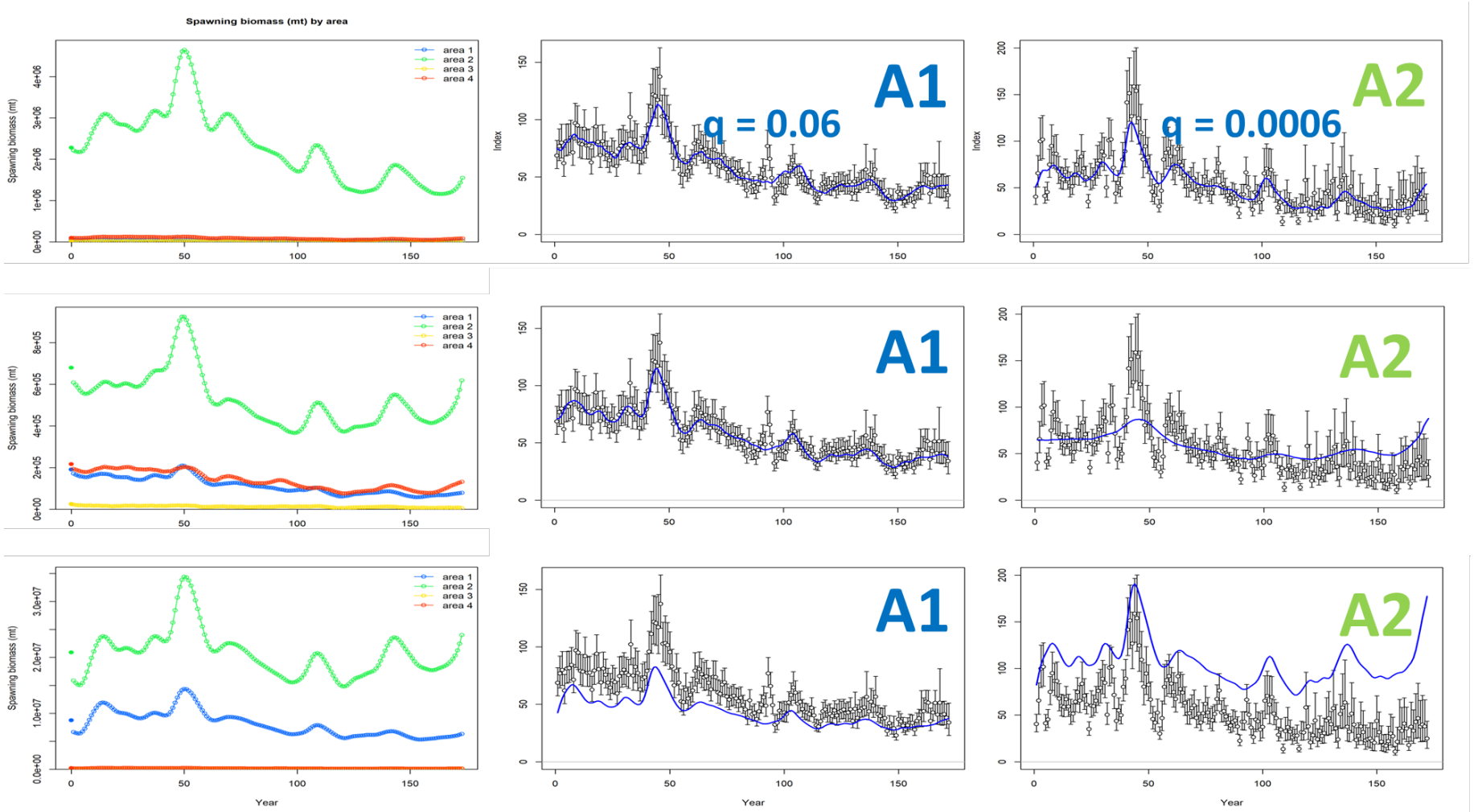

Figure 20. Time series of estimated area-specific spawning biomass (left panels) and fits to longline indices for the "Default" spatial configuration with age-dependent eastward movement rate at 16% per quarter for only juveniles (aged 3 to 8 quarters), no movement for the other ages. The top row has area-specific q and selectivities for longline, middle row has mirror q but area specific selectivities for longline, bottom row has mirror q and selectivity for longline.

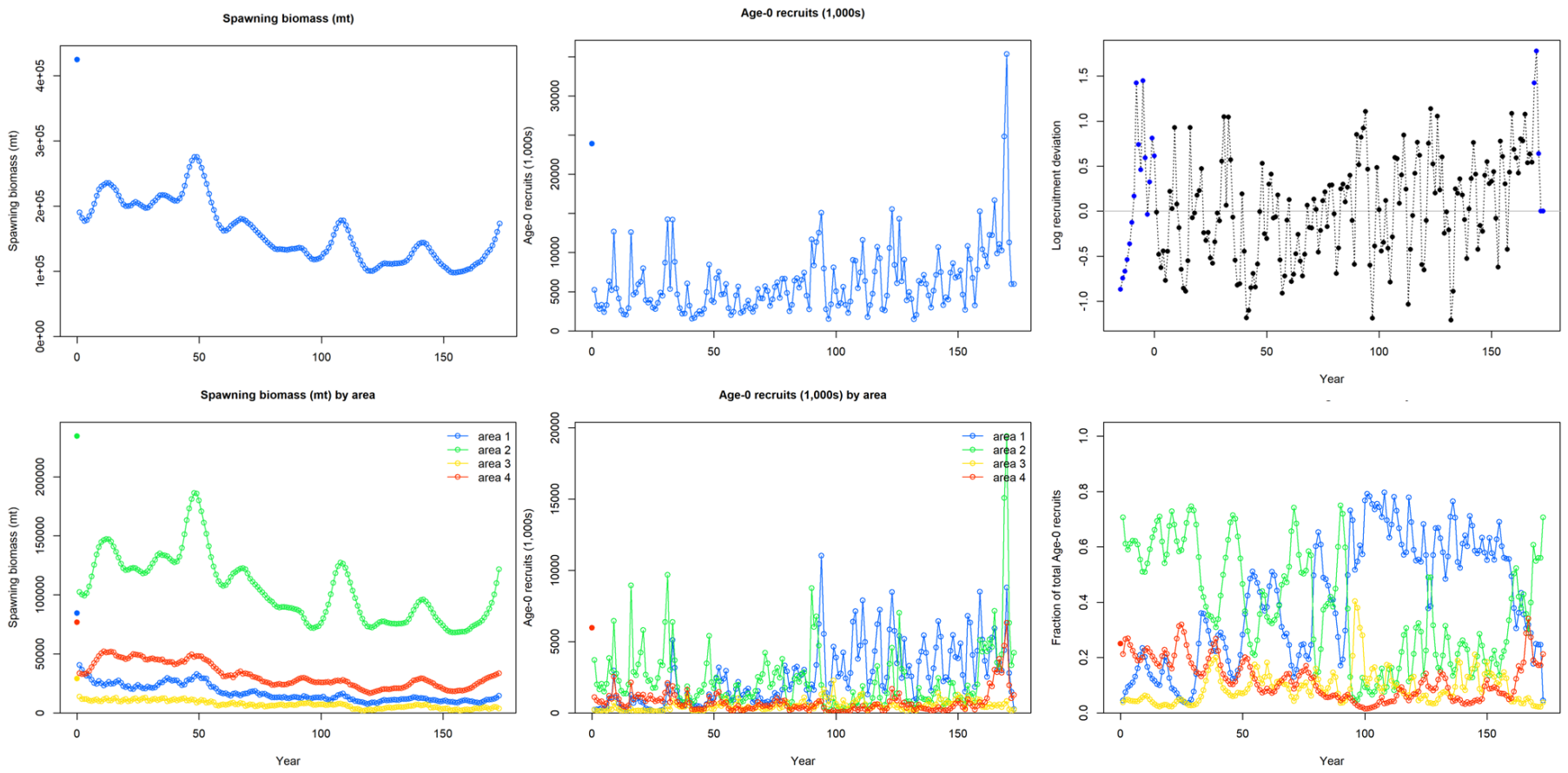

Figure 21. Estimated time-series for the "Default" spatial configuration with age-dependent eastward movement rate at 16% per quarter for only juveniles (aged 3 to 8 quarters) and 5% per quarter E-W diffusion for BET aged 15 quarters and older. Top panels from the left: Total Spawning biomass, Total age-0 recruits, Total recruitment deviates. Bottom panels from the left: Area specific time series of Spawning biomass, Age-0 recruitment and Fraction of total age-0 recruits.

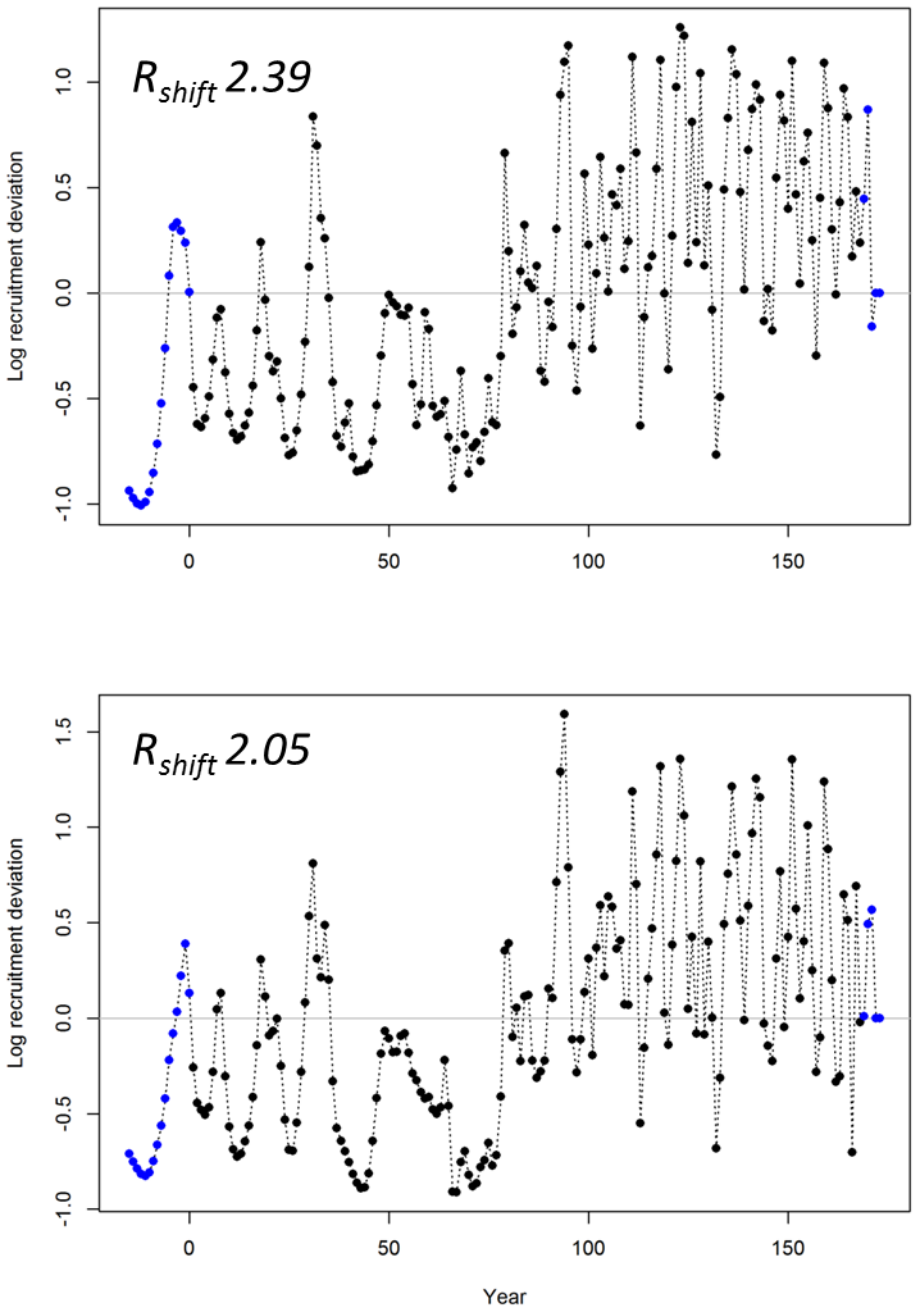

Figure 22. Area 1 (Offshore equatorial) recruitment deviations for "Alternative 1" (Top panel) and "Alternative 2" (Bottom panel). R_{shift} is the ratio of the median age-0 recruitment after the expansion of the FAD fishery over the median age-0 recruitment before the FAD expansion.

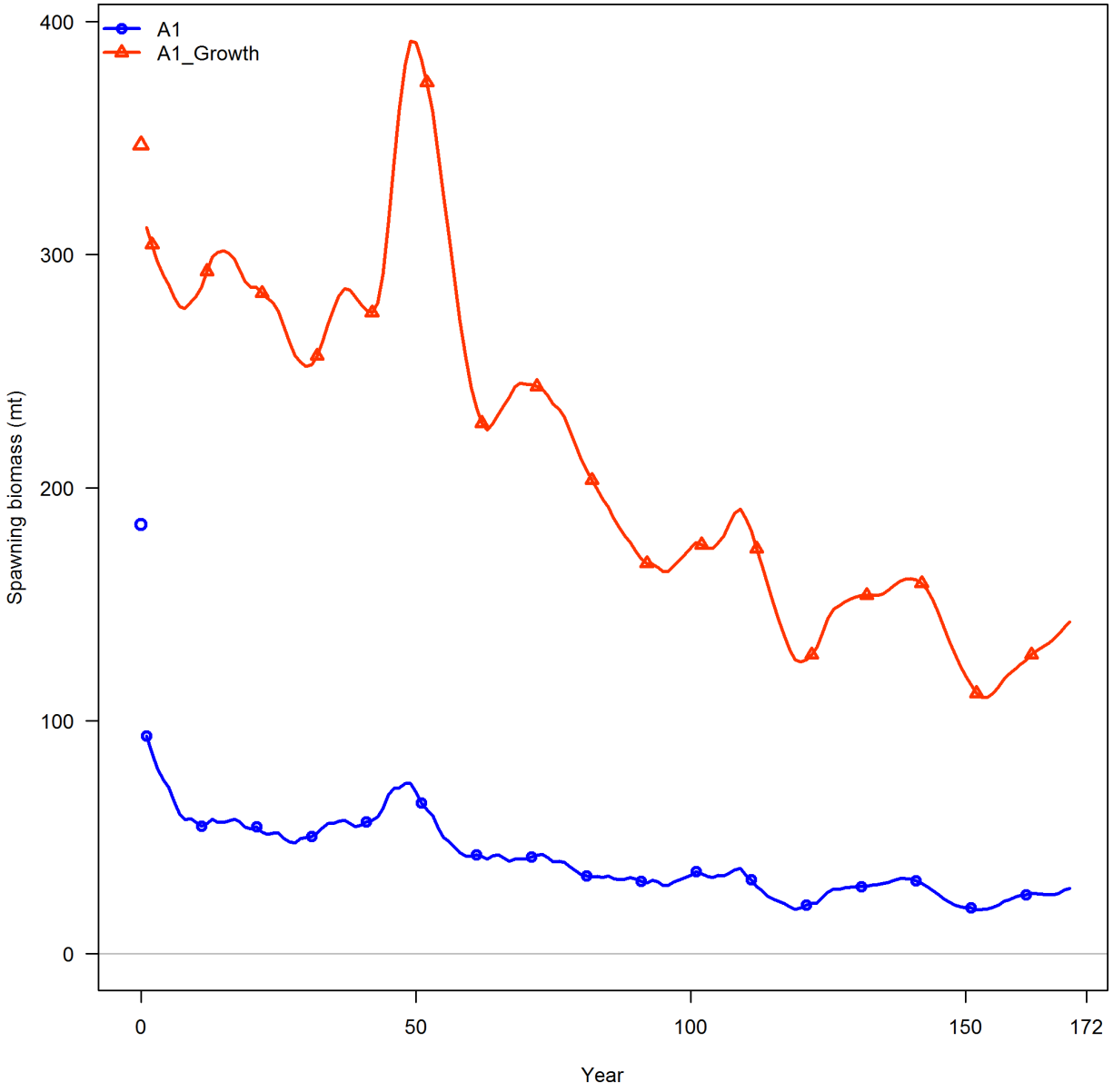

Figure 23. Time series of spawning biomass estimated for area A1 of the "Default" spatial structure with fixed growth ("A1", blue line) and estimating growth parameters Linf, K and Richards shape parameter ("A1_Growth", red line).

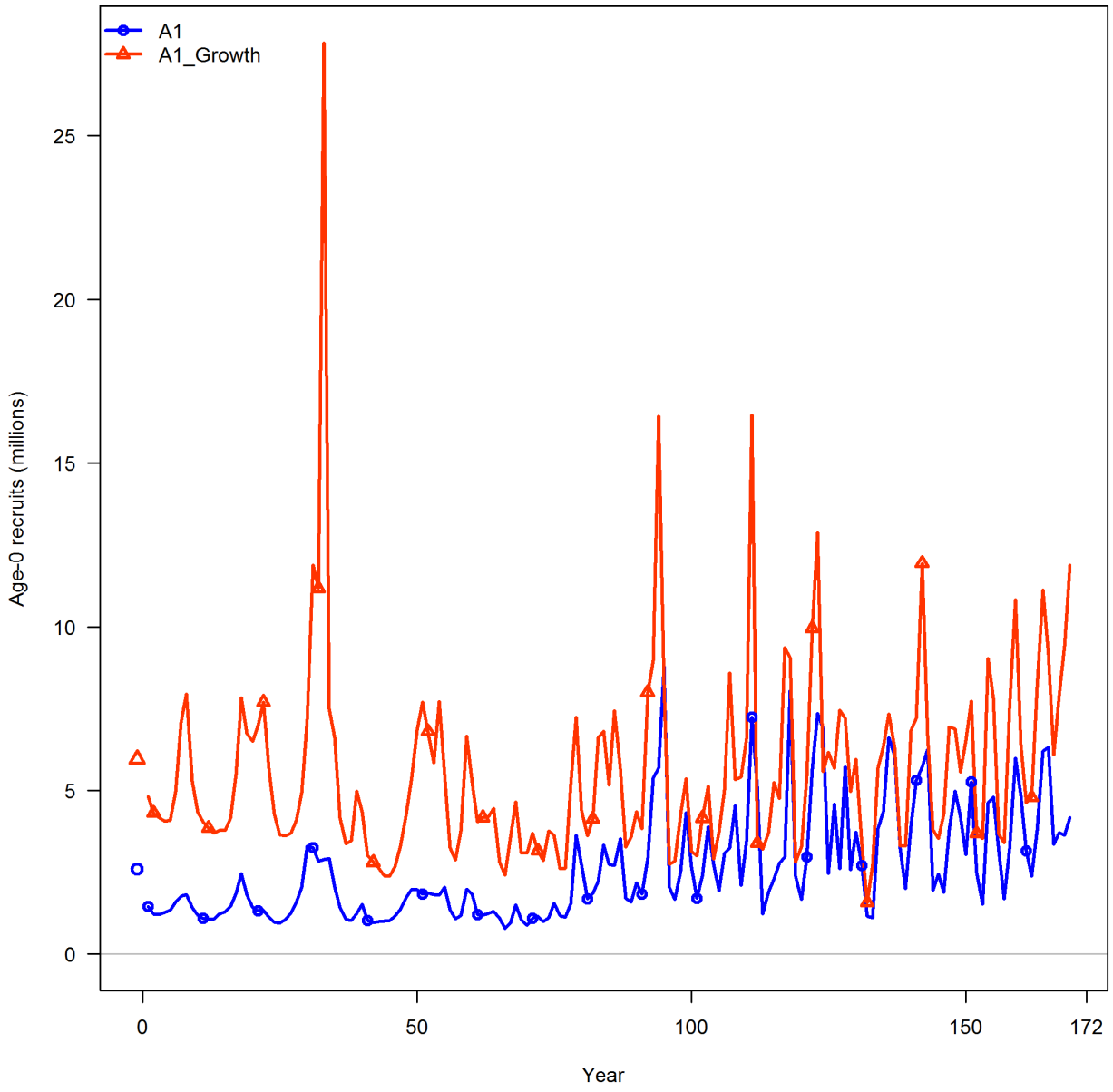

Figure 24. Time series of age-0 recruitment estimated for area A1 of the "Default" spatial structure with fixed growth ("A1", blue line) and estimating growth parameters Linf, K and Richards shape parameter ("A1_Growth", red line).

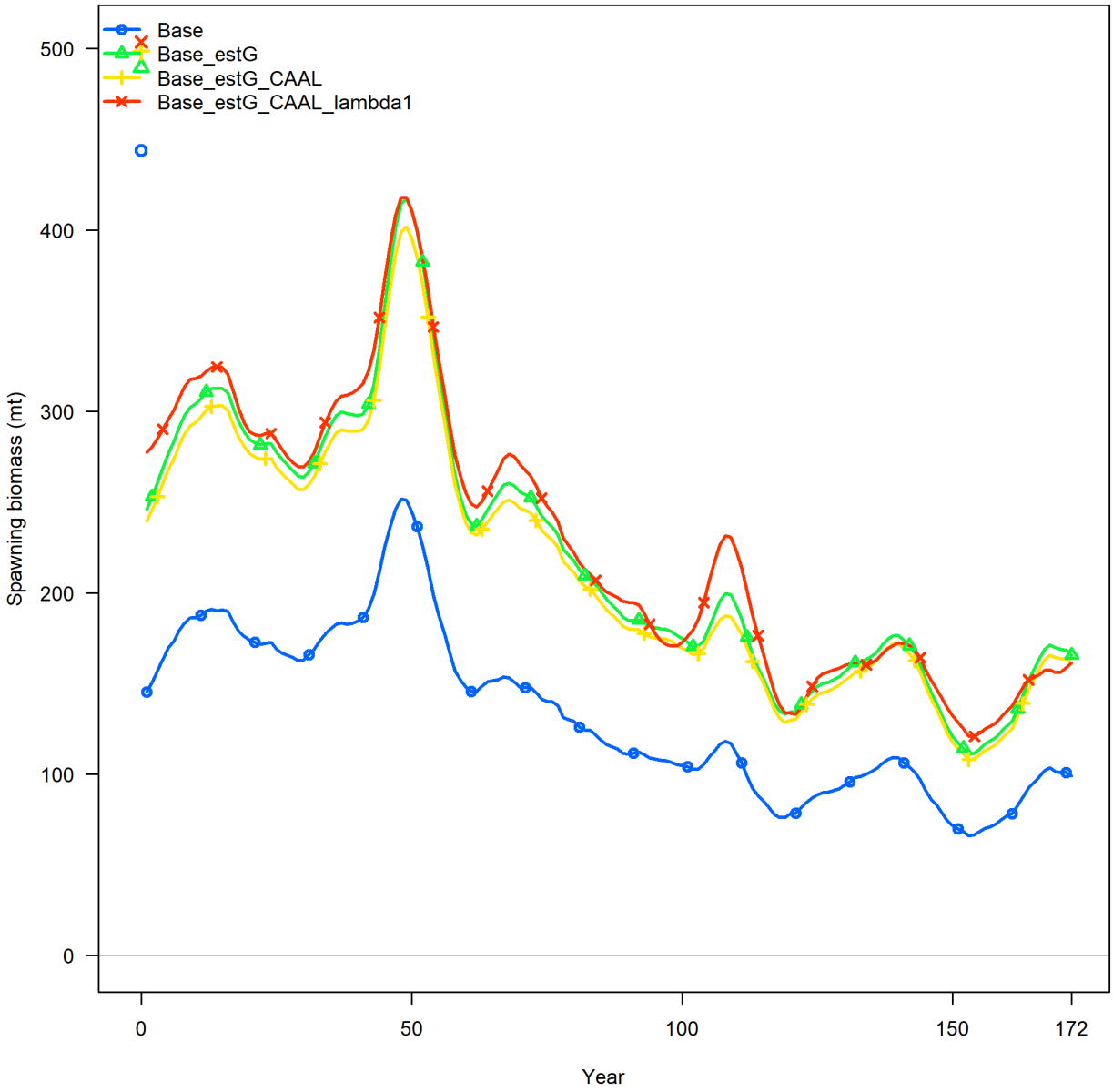

Figure 25. Alternative BET SS model runs estimating or fixing growth. "Base" is the 2018 base case BET stock assessment, "Base_estG" is identical to the "Base" but estimating L1, L2, K and the shape parameter of the Richards growth function, "Base_estG_CAAL" uses Conditional-Age-At-Length with a lambda of 1, "Base_estG_CAAL_lambda1" uses lambda 1 for all age and length composition data.

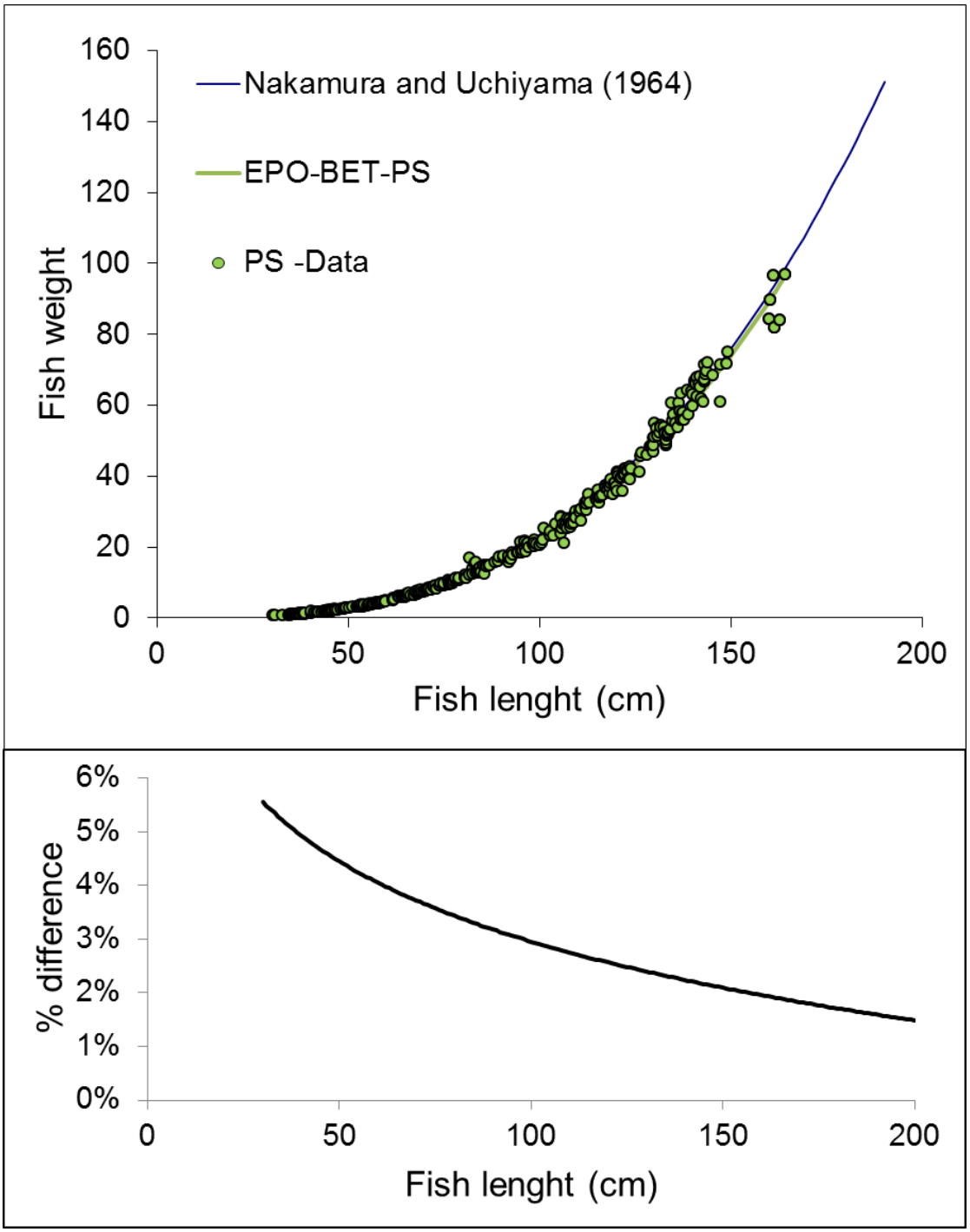

Figure 26. Top panel: Length-Weight relationships from Nakamura and Uchiyama (1964) which is based on longline caught BET (blue line) and estimated from purse-seine caught BET in the EPO (green line) paired L-W data (green circles). Bottom panel: percentage difference between longline and purse-seine caught BET.

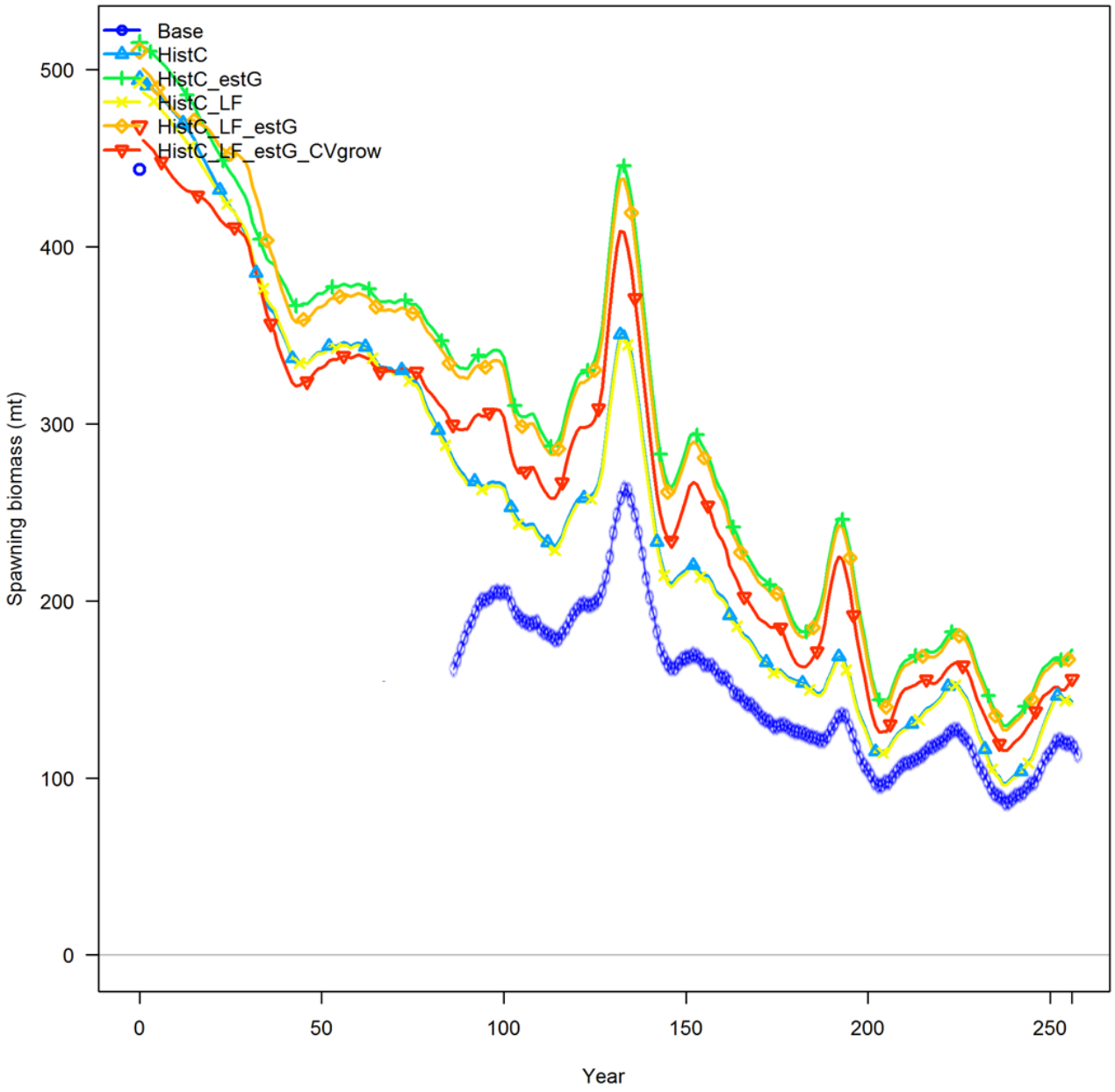

Figure 27. Alternative BET SS model runs starting in 1975 ("Base") or 1954 ("HistC"), fitting to historical longline length compositions ("LF"), estimating ("estG") or fixing growth, and estimating CVs ("CV") of growth or fixing CVs. "Base" is the 2018 base case BET stock assessment. Combinations estimating growth ("estG") use lambda of 1 for all composition data.

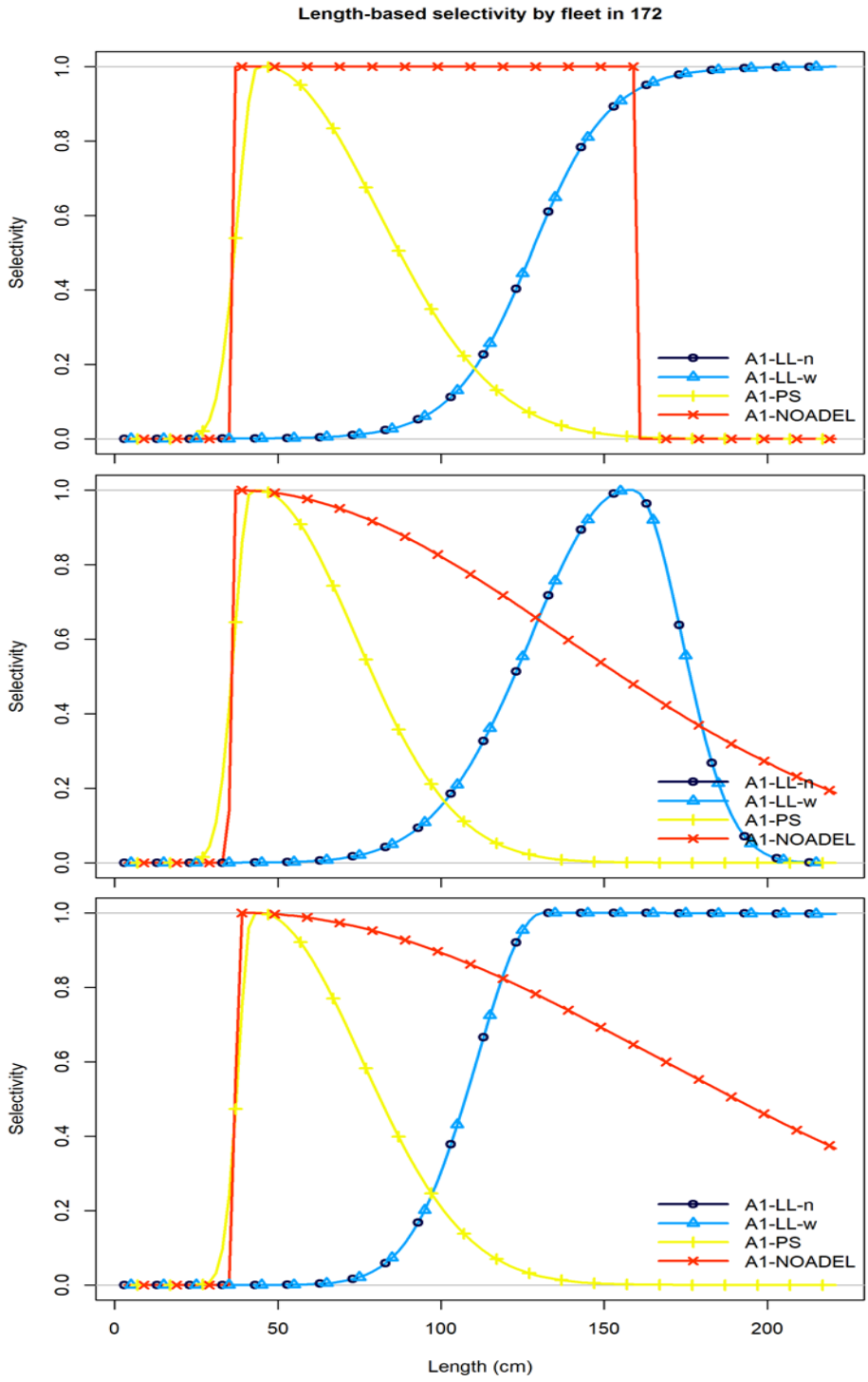

Figure 28. Estimated length-based selectivities for area A1 of the "Default" spatial structure. "LL": long-line (blue lines), "PS": purse-seine (yellow lines), "NOADEL": non-associated / dolphin sets (red lines). Top panel: base case model configuration, Middle panel: allowing dome-shaped selectivity for longline, Bottom panel: allowing dome-shaped selectivity for longline and estimating growth.

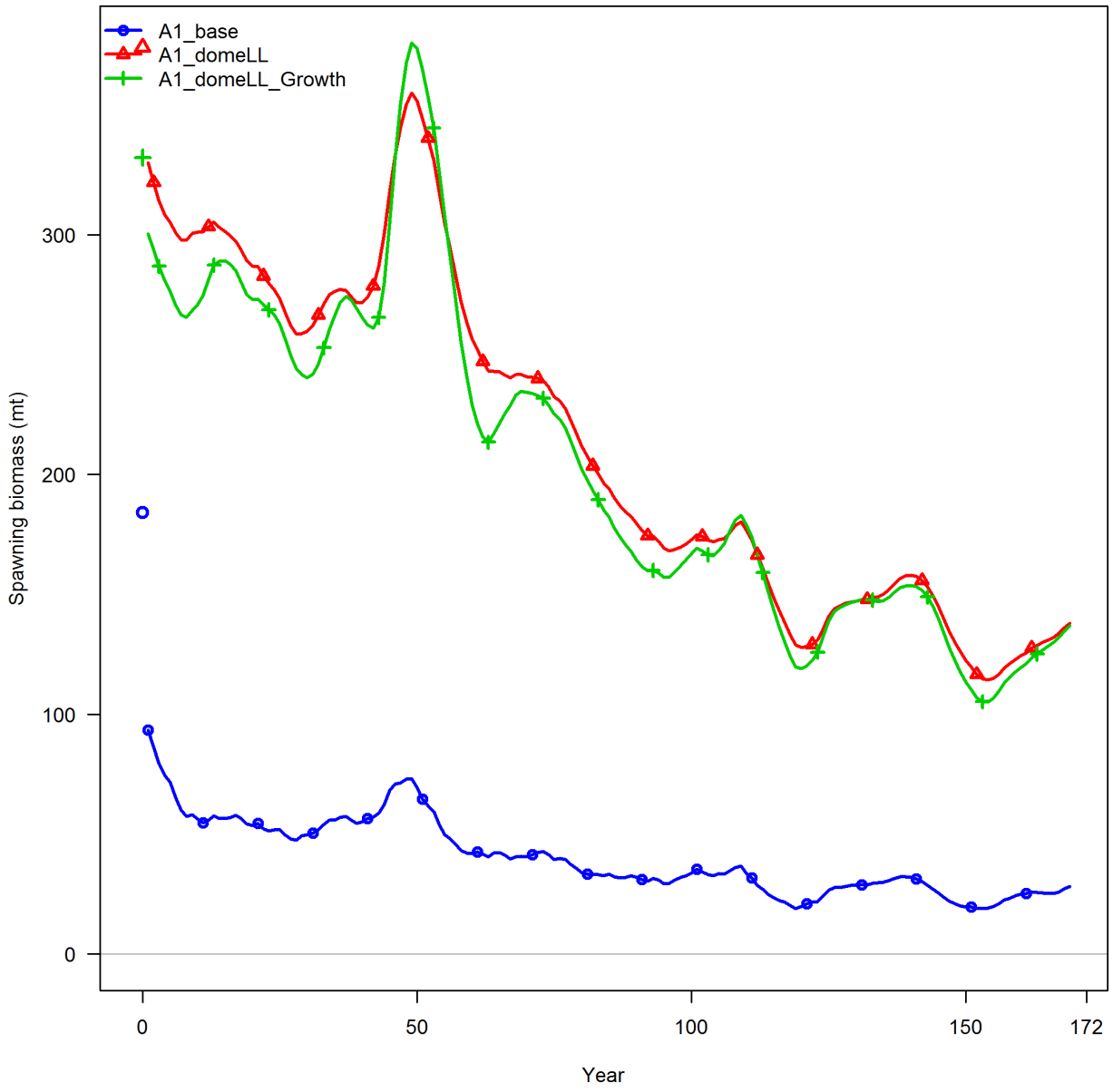

Figure 29. Estimated time series of spawning biomass for area A1 of the "Default" spatial structure. "A1_base", blue line: base case model configuration, "A1_domeLL", red line: allowing dome-shaped selectivity for longline, "A1_domeLL_Growth": allowing dome-shaped selectivity for longline and estimating growth.

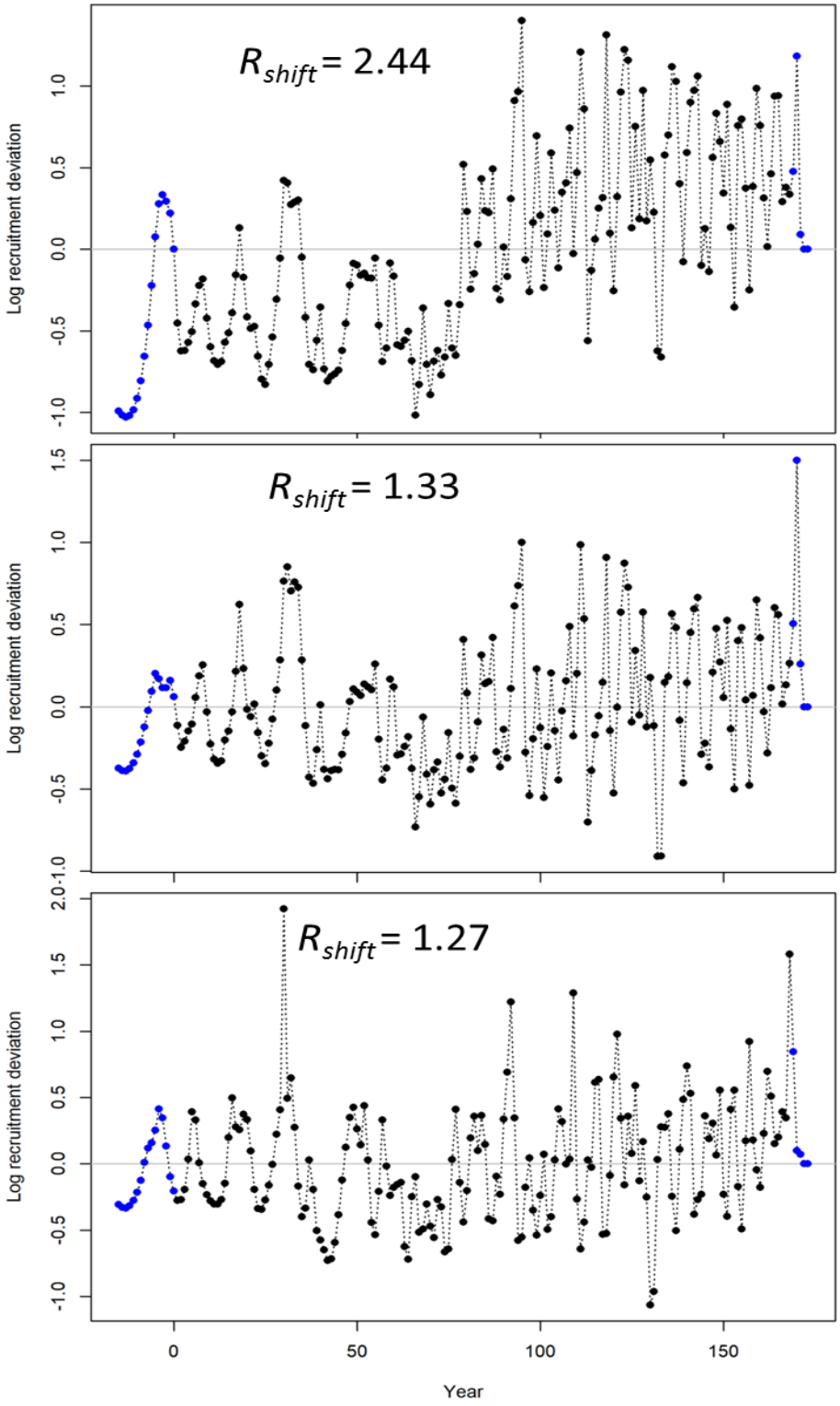

Figure 30. Age-0 recruitment deviates for alternative runs of area A1 of the "Default" spatial structure. Top panel: base case model configuration, Middle panel: allowing dome-shaped selectivity for longline, Bottom panel: allowing dome-shaped selectivity for longline and estimating growth.

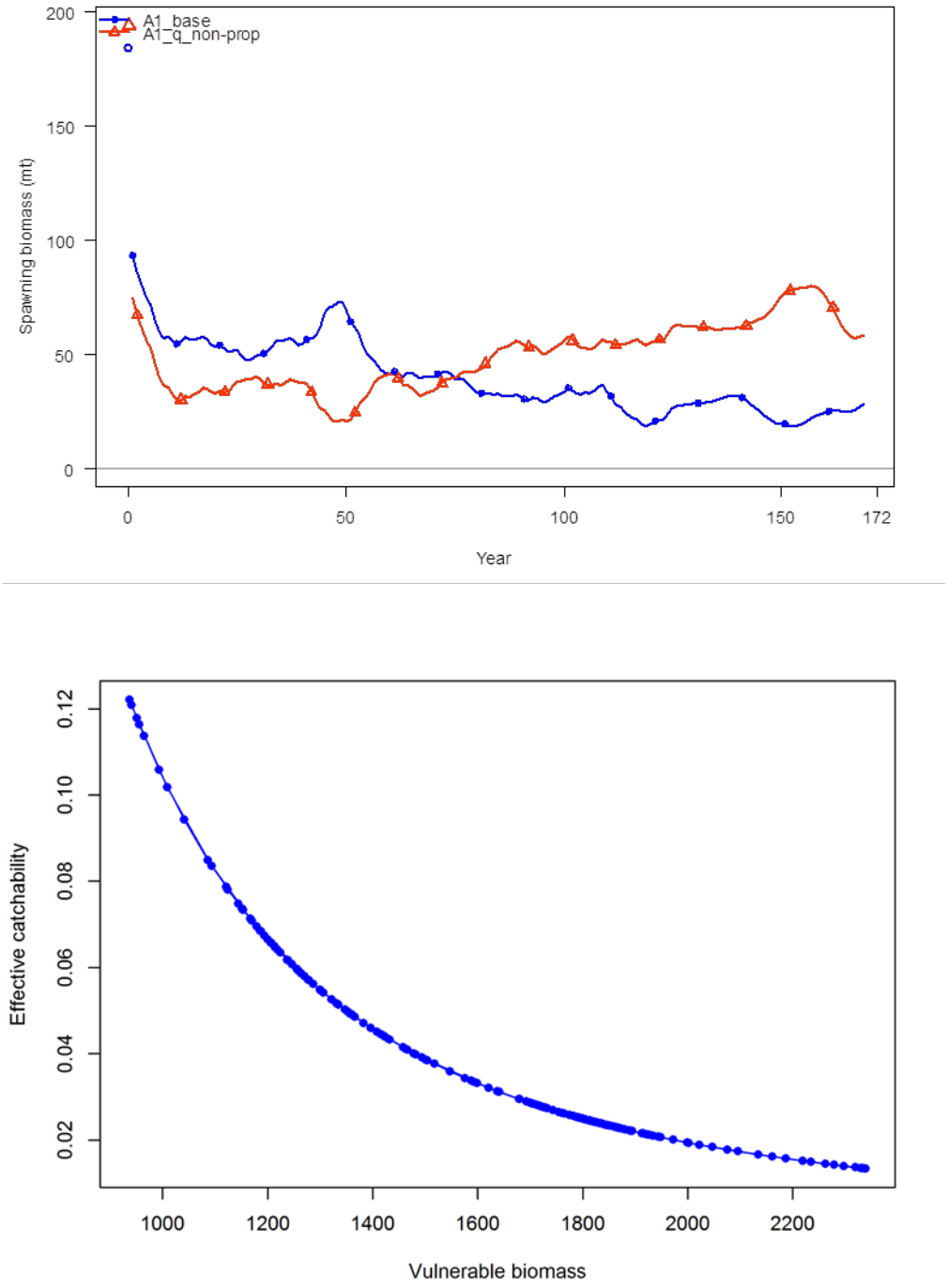

Figure 31. Top panel: Time series of estimated spawning biomass for alternative SS model runs for the area A1 of the "Default" spatial structure, "A1_base": base case model configuration, "A1_q_non-prop": estimating non-proportionality parameter for catchability (q) of the longline index. Bottom panel: effective catchability vs. vulnerable biomass for the longline fishery.

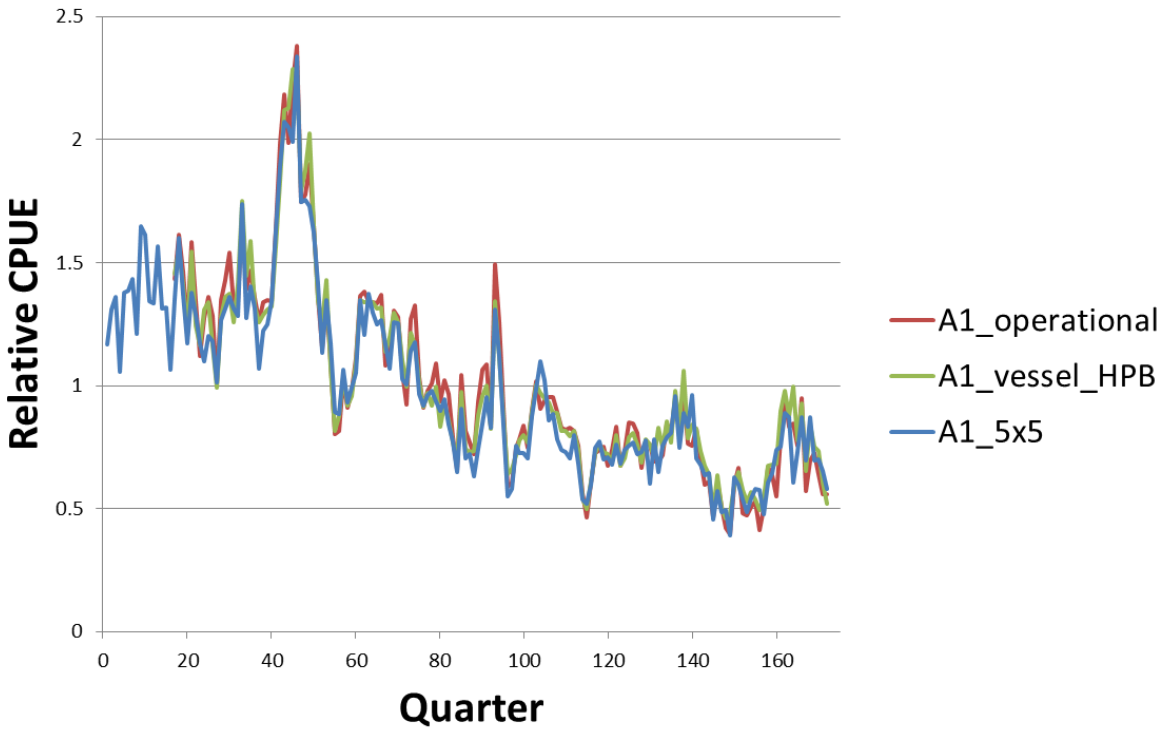

Figure 32. Relative longline indices of abundance for area A1 of the "Default" spatial structure under alternative standardizations and uses of data (From Haikun Xu, IATTC Staff). "A1_operational": uses small spatial scale operational data from longline operations, "A1_vessel_HPB": takes into account vessel effect and hook-per-basket covariate during standardization, "A1_5x5": data aggregated in a 5x5 degree grid like in the base case.